Chapter 2 Geophysical Properties of Core Samples

II-2-1. Geophysical properties and sample number

The drill core samples of four drill holes were used for measurement of the properties. The property includes magnetic susceptibility, chargeability and resistivity. The number of core samples for magnetic susceptibility is 867 while that for chargeability and resistivity is 49.

The measurement of chargeability and resistivity is conducted by time domain method. Although geophysical properties obtained by using core samples may rarely reproduce themselves, they may indicate a general trend. The properties thus obtained could be a guide for interpretation of Phase II airborne geophysical survey as well as the coming geophysical programme.

II-2-2. Equipment and sample preparation

II-2-2-1. Magnetic susceptibility

Magnetic susceptibilities were measured using a compact and light KAPAMETER at the drill sites. The specifications of the equipment is shown in Table II-2-1. The Kmetre is as highly sensitive as 0.8x10-6cgs and is designed for measurement both in rock exposures and in laboratory.

II-2-2-2. IP and resistivity

The equipment used is shown in Table II-2-1. The core samples to be measured were cut into 5 to 10 cm long and were submerged into clean water for about one day prior to measurement. The sampling time and interval to mid point against channel number are shown below.

Channel No.	4	5	6	7	8	9	10	11	12	13	14
Width(msec)	20	40	40	80	80	140	140	230	230	360	360
Mid-Point(")	60	90	130	190	270	380	520	705	935	1230	1590

Table II - 2 - 1 Equipment for Measurement of Geophysical Properties

Equipment	Maker	Type	Specifications	Num.
IP Transmitter	IRIS Instrument	IP-L Time domain O.S.C.	Output: 1 μ A～100 μ A max10V	1
IP Receiver	SCINTREX	IPR-12 Multichannel receiver	Input: 8 Channel,14 Windows Input Range : 50 μ V～14V	1
Electrode		Platinum		1
Magnetic susceptibility	Geofyzika Brno Czechoslovakia	KAPPAMETER model KT-5	Sense: 0.01×1E-3 SI Range: 0.00～999×1E-3 SI	1

II-2-3. Results and interpretation

The results of measurement are presented in Table II-2-2. The magnetic susceptibility for every metre of drill core and the detailed results of chargeability and resistivity are shown in Table II-2-3(1)-(6) and Table II-2-4 respectively. Mean values of magnetic susceptibility by drill hole and lithofacies are presented in Table II-2-5 as well as chargeability and resistivity in Table II-2-6. For processing the chargeability data the values for 12 channel; mid-point 935 msec were used.

II-2-3-1. Interpretation of magnetic susceptibility data

Magnetic susceptibility distribution of drill holes is illustrated in Fig.II-2-1. The magnetic features of each hole shown in Table II-2-2, Table II-2-4 and Figure II-2-1 were studied together with small magnetic anomalies in Fig.II-6-1 compilation and interpretation map of Phase I report.

MJNM-1: The susceptibility is comparatively high at the lower part of calcrete and upper part of dolomite just underlying the unconformity where the higher the susceptibility may be, the more cores are reddish. The cores show brecciation and veinning with matrix of reddish material resulted from comparatively abundant iron oxides. The susceptibility is low at the other lower dolomite facies and the mineralised sections giving 0.01 to 0.02x10-3SI. Therefore the small magnetic anomalies could be originated from iron oxides embedded around 70 to 90 metre deep.

MJNM-2: Higher susceptibility values come from surface calcrete and shales at around 150 and 180 metre deep as well as lower dolomite however, no notably high values were observed. The isolated magnetic anomaly or magnetic lineament in the vicinity of the hole possibly resulted from subsurface shale which has comparatively high susceptibility.

MJNM-3: The calcrete is thin but has slightly high magnetic susceptibility. The susceptibility is almost low in the underlying dolomitic formation, in which the fractures filled with small amount of iron oxides, it is high. But origin of the magnetic anomaly could not be detected because of discontinuous high susceptibility.

MJNM-4: The overlying calcrete shows higher magnetic susceptibility compared to the other formations. Local magnetite grain 1 m/m cubic in size causes remarkably high susceptibility in particular. The magnetic minerals included in calcrete are thus believed to result in the aeromagnetic anomaly.

Table II - 2 - 2 Result of Geophysical Test of Core Samples

Sample No.	Depth m	Rock, Mineral name	Physical properties		
			Mag.sus. *1E-3 SI	Resistivity Ω·m	IP(M12) mV/V
MJNM-1-1	1.10	Calcrete	0.02	989	0.30
MJNM-1-2	20.00	Calcrete	0.07	2,322	0.24
MJNM-1-3	40.00	Sandy Calcrete	0.05	247	0.50
MJNM-1-4	61.00	Coarse pebbles	0.11	289	4.40
MJNM-1-5	78.90	Coarse pebbles	0.55	390	0.52
MJNM-1-6	99.90	Grainite	0.03	423	0.86
MJNM-1-7	111.58	Sphalerite Galena disseminated	0.02	9,440	3.33
MJNM-1-8	112.30	Galena ore	0.02	9,971	2.84
MJNM-1-9	120.05	Dolomite	0.03	859	1.26
MJNM-1-10	139.65	Grey dolomite	0.02	2,491	0.29
MJNM-1-11	160.00	Massive dolomite	0.02	1,089	1.82
MJNM-1-12	180.16	Dolomite	0.02	1,453	1.10
MJNM-1-13	200.00	Dolomite	0.02	908	0.25
MJNM-1-15	220.00	Dolomite	0.01	1,535	0.23
MJNM-1-16	239.80	Dolomite	0.02	1,554	0.39
MJNM-1-17	259.90	Dolomite	0.02	1,597	0.25
MJNM-1-18	245.75	Sphalerite pod	0.02	576	1.21
MJNM-1-19	279.00	Dolomite	0.01	1,503	0.43
MJNM-1-20	299.90	Dolomite	0.01	1,545	0.38
MJNM-2-1	3.00	Calcrete	0.01	961	1.36
MJNM-2-2	30.25	Calcrete	0.02	1,800	2.50
MJNM-2-3	60.70	Brecciated Calcrete	0.04	2,381	2.89
MJNM-2-4	81.00	Dolomite	0.01	14,646	1.33
MJNM-2-5	99.90	Dark grey dolomite	0.01	8,158	1.16
MJNM-2-6	115.00	Black dolomitic shale	0.02	24,827	0.35
MJNM-2-7	151.00	Black dolomitic shale	0.13	805	1.37
MJNM-2-8	185.00	Shale & Dolomite	0.15	244	2.42
MJNM-2-9	195.10	Oolitic chert	0.02	26,726	0.15
MJNM-2-10	227.70	Sandstone	0.05	17,569	0.13
MJNM-2-11	251.15	Dolomite	0.09	12,045	1.28
MJNM-2-12	272.33	Massive dolomite	0.55	19,755	1.10
MJNM-2-13	298.40	Massive dolomite	0.11	5,553	3.56
MJNM-3-1	4.00	Calcrete	0.05	1,232	2.94
MJNM-3-2	29.80	Massive dolomite	0.02	38,567	0.34
MJNM-3-3	60.00	Massive dolomite	0.03	2,289	0.63
MJNM-3-4	75.52	Calcareous sandstone	0.02	500	0.11
MJNM-3-5	91.05	Dolomite	0.02	4,082	0.14
MJNM-3-6	119.75	Dolomite	0.07	37,988	3.00
MJNM-3-7	149.20	Med.-fine dolomite	0.02	26,039	0.11
MJNM-4-1	9.50	Dark grey dolomite	0.02	24,721	0.10
MJNM-4-2	30.80	Grey fine dolomite	0.13	25,175	0.39
MJNM-4-3	60.70	Black sandy shale	0.03	7,654	1.51
MJNM-4-4	94.00	Cream limestone	0.03	3,360	4.68
MJNM-4-5	119.40	Druse rich dolomite	0.02	3,797	5.11
MJNM-4-6	149.90	Dolomite with sericite layer	0.03	1,793	0.76

Table II - 2 - 3 (1) Magnetic Susceptibility of Drill Cores

Depth	MJNM-1		MJNM-2		MJNM-3			MJNM-4	
	Mag.sus.	Lithology	Mag.sus.	Lithology	Mag.sus.	Lithology		Mag.sus.	Lithology
(m)	*1E-3(SI)	No.	*1E-3(SI)	No.	*1E-3(SI)	No.		*1E-3(SI)	No.
0			0.05	2	Calcrete				
1	0.02	1	Calcrete						
2	0.01	1	Calcrete	0.03	2	Calcrete			
3	0.01	1	Calcrete	0.01	2	Calcrete	0.05	1	Calcrete
4	0.02	1	Calcrete				0.05	1	Calcrete
5	0.03	1	Calcrete	0.02	2	Calcrete	0.03	1	Calcrete	0.02	2 Calcrete
6	0.05	1	Calcrete	0.03	2	Calcrete	0.10	1	Calcrete	0.02	3 Dolomite
7	0.05	1	Calcrete	0.01	2	Calcrete	0.10	1	Calcrete	0.07	3 Dolomite
8	0.05	1	Calcrete	0.03	2	Calcrete	0.07	1	Calcrete	0.09	3 Dolomite
9	0.05	1	Calcrete	0.03	2	Calcrete	0.02	1	Calcrete	0.04	3 Dolomite
10	0.05	1	Calcrete	0.03	2	Calcrete	0.02	1	Calcrete	0.02	3 Dolomite
11	0.05	1	Calcrete	0.01	2	Calcrete	0.02	1	Calcrete	0.04	3 Dolomite
12	0.05	1	Calcrete	0.07	2	Calcrete	0.02	3	Dolomite	0.04	3 Dolomite
13	0.05	1	Calcrete	0.01	2	Calcrete	0.02	3	Dolomite	0.02	3 Dolomite
14	0.05	1	Calcrete	0.02	2	Calcrete	0.03	3	Dolomite	0.04	3 Dolomite
15	0.05	1	Calcrete	0.01	2	Calcrete	0.02	3	Dolomite	0.04	3 Dolomite
16	0.07	1	Calcrete	0.01	2	Calcrete	0.02	3	Dolomite	0.04	3 Dolomite
17	0.03	1	Calcrete	0.01	2	Calcrete	0.05	4	Dolomite	0.04	3 Dolomite
18	0.07	1	Calcrete	0.01	2	Calcrete	0.02	3	Dolomite	0.02	3 Dolomite
19	0.07	1	Calcrete	0.05	2	Calcrete	0.02	3	Dolomite	0.02	3 Dolomite
20	0.07	1	Calcrete	0.01	2	Calcrete	0.02	3	Dolomite	0.02	3 Dolomite
21	0.03	1	Calcrete	0.01	2	Calcrete	0.02	3	Dolomite	0.04	3 Dolomite
22	0.03	1	Calcrete	0.01	2	Calcrete	0.02	3	Dolomite	0.04	11 Shale
23	0.03	1	Calcrete	0.01	1	Calcrete	0.02	3	Dolomite	0.05	3 Dolomite
24	0.03	1	Calcrete	0.01	1	Calcrete	0.02	3	Dolomite	0.04	11 Shale
25	0.05	1	Calcrete	0.01	1	Calcrete	0.02	3	Dolomite	0.05	3 Dolomite
26	0.03	1	Calcrete	0.02	1	Calcrete	0.02	3	Dolomite		
27	0.03	1	Calcrete	0.02	1	Calcrete	0.02	3	Dolomite		
28	0.03	1	Calcrete	0.02	1	Calcrete	0.02	3	Dolomite	0.05	3 Dolomite
29	0.05	1	Calcrete	0.02	1	Calcrete	0.02	3	Dolomite	0.04	3 Dolomite
30	0.05	1	Calcrete	0.02	1	Calcrete	0.02	3	Dolomite	0.07	3 Dolomite
31	0.05	1	Calcrete	0.03	1	Calcrete	0.02	3	Dolomite	0.13	3 Dolomite
32	0.07	1	Calcrete	0.01	1	Calcrete	0.02	3	Dolomite	0.02	3 Dolomite
33	0.05	1	Calcrete	0.01	1	Calcrete	0.02	3	Dolomite	0.04	3 Dolomite
34	0.05	1	Calcrete	0.03	1	Calcrete	0.02	3	Dolomite	0.04	3 Dolomite
35	0.07	2	Calcrete	0.05	1	Calcrete	0.02	3	Dolomite	0.02	10 Chert
36	0.03	2	Calcrete	0.03	1	Calcrete	0.02	3	Dolomite		
37	0.03	2	Calcrete	0.05	1	Calcrete	0.02	3	Dolomite		
38	0.03	2	Calcrete	0.05	1	Calcrete	0.02	3	Dolomite	0.05	3 Dolomite
39	0.05	2	Calcrete	0.03	2	Calcrete	0.02	3	Dolomite		
40	0.05	2	Calcrete	0.03	2	Calcrete	0.02	3	Dolomite		
41	0.05	2	Calcrete	0.02	2	Calcrete	0.02	3	Dolomite		
42	0.08	2	Calcrete	0.05	2	Calcrete	0.02	3	Dolomite		
43	0.07	2	Calcrete	0.05	2	Calcrete	0.03	3	Dolomite	0.04	3 Dolomite
44	0.07	2	Calcrete	0.05	2	Calcrete	0.02	3	Dolomite		
45	0.08	2	Calcrete	0.04	2	Calcrete	0.02	3	Dolomite		
46	0.07	2	Calcrete	0.04	2	Calcrete	0.02	3	Dolomite		
47	0.07	2	Calcrete	0.04	2	Calcrete	0.03	11	Shale		
48	0.08	2	Calcrete	0.05	2	Calcrete	0.03	11	Shale	0.04	3 Dolomite
49	0.13	2	Calcrete	0.04	2	Calcrete	0.03	7	Dolomite		
50	0.05	2	Calcrete	0.09	2	Calcrete	0.03	7	Dolomite		

Table II - 2 - 3 (2) Magnetic Susceptibility of Drill Cores

Depth (m)	MJNM-1 Mag.sus. *1E-3(SI)	MJNM-1 No.	MJNM-1 Lithology	MJNM-2 Mag.sus. *1E-3(SI)	MJNM-2 No.	MJNM-2 Lithology	MJNM-3 Mag.sus. *1E-3(SI)	MJNM-3 No.	MJNM-3 Lithology	MJNM-4 Mag.sus. *1E-3(SI)	MJNM-4 No.	MJNM-4 Lithology
51	0.10	1	Calcrete	0.07	2	Calcrete	0.02	3	Dolomite			
52	0.07	1	Calcrete	0.07	2	Calcrete	0.03	3	Dolomite			
53	0.08	1	Calcrete	0.07	2	Calcrete	0.02	3	Dolomite	0.01	11	Shale
54	0.10	1	Calcrete	0.09	2	Calcrete	0.02	3	Dolomite			
55	0.10	1	Calcrete	0.09	2	Calcrete	0.03	3	Dolomite			
56	0.15	1	Calcrete	0.05	2	Calcrete	0.02	3	Dolomite			
57	0.13	2	Calcrete	0.05	2	Calcrete	0.02	3	Dolomite	0.04	16	Shale⁄Dol
58	0.07	2	Calcrete	0.02	2	Calcrete	0.02	3	Dolomite			
59	0.11	1	Calcrete	0.07	2	Calcrete	0.02	3	Dolomite			
60	0.10	1	Calcrete	0.05	2	Calcrete	0.03	3	Dolomite	0.01	16	Shale⁄Dol
61	0.11	2	Calcrete	0.04	2	Calcrete	0.01	3	Dolomite	0.03	16	Shale⁄Dol
62	0.08	2	Calcrete	0.02	3	Dolomite	0.07	3	Dolomite	0.03	4	Dolomite
63	0.10	2	Calcrete	0.01	3	Dolomite	0.03	3	Dolomite	0.02	4	Dolomite
64	0.13	2	Calcrete	0.02	3	Dolomite	0.01	3	Dolomite	0.02	4	Dolomite
65	0.07	2	Calcrete	0.36	3	Dolomite	0.02	3	Dolomite	0.01	4	Dolomite
66	0.08	2	Calcrete	0.02	3	Dolomite	0.02	3	Dolomite	0.02	4	Dolomite
67	0.08	2	Calcrete	0.01	3	Dolomite	0.02	3	Dolomite	0.02	3	Dolomite
68	0.07	2	Calcrete	0.01	3	Dolomite	0.03	3	Dolomite	0.03	3	Dolomite
69	0.11	2	Calcrete	0.01	3	Dolomite	0.01	3	Dolomite	0.02	3	Dolomite
70	0.16	2	Calcrete	0.02	12	Dol.Chert	0.02	3	Dolomite	0.01	3	Dolomite
71	0.16	2	Calcrete	0.04	3	Dolomite	0.02	3	Dolomite	0.02	3	Dolomite
72	0.18	2	Calcrete	0.02	3	Dolomite	0.02	3	Dolomite	0.03	3	Dolomite
73	0.18	2	Calcrete	0.02	3	Dolomite	0.02	3	Dolomite	0.03	3	Dolomite
74	0.13	2	Calcrete	0.02	3	Dolomite	0.02	3	Dolomite	0.03	3	Dolomite
75	0.20	2	Calcrete	0.04	3	Dolomite	0.02	15	Sandstone	0.01	3	Dolomite
76	0.10	2	Calcrete	0.05	3	Dolomite	0.02	15	Sandstone	0.11	3	Dolomite
77	0.13	2	Calcrete	0.05	3	Dolomite	0.02	15	Sandstone	0.02	11	Shale
78	0.36	2	Calcrete	0.01	3	Dolomite	0.01	3	Dolomite	0.03	11	Shale
79	0.55	2	Calcrete	0.01	3	Dolomite	0.03	3	Dolomite	0.02	3	Dolomite
80	0.33	2	Calcrete	0.01	3	Dolomite	0.03	3	Dolomite	0.01	3	Dolomite
81	0.49	2	Calcrete	0.01	3	Dolomite	0.01	3	Dolomite	0.02	3	Dolomite
82	0.20	2	Calcrete	0.04	3	Dolomite	0.01	3	Dolomite	0.02	3	Dolomite
83	0.10	2	Calcrete	0.01	3	Dolomite	0.02	3	Dolomite	0.02	3	Dolomite
84	0.07	2	Calcrete	0.02	3	Dolomite	0.02	3	Dolomite	0.02	3	Dolomite
85	0.15	2	Calcrete	0.04	3	Dolomite	0.03	3	Dolomite	0.01	3	Dolomite
86	0.02	3	Dolomite	0.02	3	Dolomite	0.01	3	Dolomite	0.03	3	Dolomite
87	0.02	3	Dolomite	0.01	3	Dolomite	0.01	3	Dolomite	0.03	3	Dolomite
88	0.02	3	Dolomite	0.02	3	Dolomite	0.02	3	Dolomite	0.01	3	Dolomite
89	0.16	3	Dolomite	0.01	3	Dolomite	0.03	3	Dolomite	0.02	3	Dolomite
90	0.03	3	Dolomite	0.01	3	Dolomite	0.03	3	Dolomite	0.01	3	Dolomite
91	0.02	4	Dolomite	0.01	3	Dolomite	0.02	3	Dolomite	0.03	5	Dolomite
92	0.02	11	Shale	0.01	3	Dolomite	0.01	3	Dolomite	0.02	5	Dolomite
93	0.02	11	Shale	0.01	3	Dolomite	0.02	3	Dolomite	0.02	4	Dolomite
94	0.02	11	Shale	0.01	3	Dolomite	0.02	3	Dolomite	0.03	3	Dolomite
95	0.03	5	Dolomite	0.02	3	Dolomite	0.02	3	Dolomite	0.01	3	Dolomite
96	0.05	5	Dolomite	0.01	3	Dolomite	0.02	3	Dolomite	0.03	3	Dolomite
97	0.02	5	Dolomite	0.01	3	Dolomite	0.02	3	Dolomite			
98	0.02	5	Dolomite	0.01	3	Dolomite	0.02	3	Dolomite			
99	0.03	5	Dolomite	0.01	3	Dolomite	0.02	3	Dolomite			
100	0.03	13	Mineraliza.	0.01	3	Dolomite	0.03	3	Dolomite	0.01	3	Dolomite

Table II - 2 - 3 (3) Magnetic Susceptibility of Drill Cores

Depth	MJNM-1		MJNM-2		MJNM-3		MJNM-4	
	Mag.sus.	Lithology	Mag.sus.	Lithology	Mag.sus.	Lithology	Mag.sus.	Lithology
(m)	*1E-3(SI)	No.	*1E-3(SI)	No.	*1E-3(SI)	No.	*1E-3(SI)	No.
101	0.02	13 Mineraliza.	0.02	11 Shale	0.02	3 Dolomite	0.07	3 Dolomite
102	0.02	13 Mineraliza.	0.01	11 Shale	0.02	3 Dolomite	0.02	3 Dolomite
103	0.02	13 Mineraliza.	0.01	11 Shale	0.01	3 Dolomite	0.03	3 Dolomite
104	0.02	13 Mineraliza.	0.01	11 Shale	0.02	3 Dolomite	0.03	5 Dolomite
105	0.02	3 Dolomite	0.01	11 Shale	0.02	3 Dolomite	0.02	5 Dolomite
106	0.02	3 Dolomite	0.01	11 Shale	0.02	3 Dolomite	0.02	5 Dolomite
107	0.02	3 Dolomite	0.01	11 Shale	0.02	3 Dolomite	0.03	5 Dolomite
108	0.01	3 Dolomite	0.01	11 Shale	0.02	3 Dolomite	0.03	5 Dolomite
109	0.02	3 Dolomite	0.01	11 Shale	0.02	3 Dolomite	0.02	5 Dolomite
110	0.03	3 Dolomite	0.01	11 Shale	0.02	3 Dolomite	0.02	11 Shale
111	0.02	3 Dolomite	0.01	11 Shale	0.02	3 Dolomite	0.02	11 Shale
112	0.02	3 Dolomite	0.02	11 Shale	0.01	3 Dolomite	0.03	11 Shale
113	0.01	3 Dolomite	0.02	11 Shale	0.02	3 Dolomite	0.03	11 Shale
114	0.02	3 Dolomite	0.02	11 Shale	0.02	3 Dolomite	0.03	11 Shale
115	0.02	3 Dolomite	0.02	11 Shale	0.03	3 Dolomite	0.02	11 Shale
116	0.02	3 Dolomite	0.02	11 Shale	0.02	3 Dolomite	0.02	11 Shale
117	0.02	3 Dolomite	0.02	11 Shale	0.02	3 Dolomite	0.01	4 Dolomite
118	0.01	3 Dolomite	0.02	11 Shale	0.02	10 Chert	0.01	3 Dolomite
119	0.02	3 Dolomite	0.02	11 Shale	0.05	7 Dolomite	0.02	3 Dolomite
120	0.03	4 Dolomite	0.04	11 Shale	0.07	3 Dolomite	0.02	3 Dolomite
121	0.02	4 Dolomite	0.01	11 Shale	0.03	5 Dolomite	0.03	3 Dolomite
122	0.02	3 Dolomite	0.02	11 Shale	0.01	5 Dolomite	0.02	3 Dolomite
123	0.01	3 Dolomite	0.01	11 Shale	0.02	5 Dolomite	0.03	3 Dolomite
124	0.11	3 Dolomite	0.01	11 Shale	0.02	5 Dolomite	0.03	3 Dolomite
125	0.02	4 Dolomite	0.01	11 Shale	0.02	5 Dolomite	0.02	3 Dolomite
126	0.01	4 Dolomite	0.02	11 Shale	0.01	5 Dolomite	0.03	4 Dolomite
127	0.02	4 Dolomite	0.01	11 Shale	0.02	5 Dolomite	0.02	4 Dolomite
128	0.02	4 Dolomite	0.04	11 Shale	0.02	5 Dolomite	0.03	4 Dolomite
129	0.01	5 Dolomite	0.01	11 Shale	0.02	5 Dolomite	0.03	4 Dolomite
130	0.02	5 Dolomite	0.01	11 Shale	0.03	3 Dolomite	0.03	4 Dolomite
131	0.02	4 Dolomite	0.01	11 Shale	0.02	3 Dolomite	0.02	4 Dolomite
132	0.01	4 Dolomite	0.01	11 Shale	0.02	3 Dolomite	0.03	4 Dolomite
133	0.01	4 Dolomite	0.02	11 Shale	0.02	3 Dolomite	0.03	4 Dolomite
134	0.02	4 Dolomite	0.01	11 Shale	0.02	3 Dolomite	0.03	4 Dolomite
135	0.01	4 Dolomite	0.02	11 Shale	0.03	3 Dolomite	0.01	4 Dolomite
136	0.02	5 Dolomite	0.02	11 Shale	0.02	3 Dolomite	0.02	4 Dolomite
137	0.02	5 Dolomite	0.01	11 Shale	0.01	3 Dolomite	0.02	4 Dolomite
138	0.02	5 Dolomite	0.01	11 Shale	0.02	3 Dolomite	0.02	4 Dolomite
139	0.02	5 Dolomite	0.01	11 Shale	0.03	3 Dolomite	0.02	4 Dolomite
140	0.02	5 Dolomite	0.04	11 Shale	0.02	3 Dolomite	0.03	4 Dolomite
141	0.01	3 Dolomite	0.07	11 Shale	0.01	3 Dolomite	0.02	4 Dolomite
142	0.02	3 Dolomite	0.11	11 Shale	0.01	3 Dolomite	0.02	4 Dolomite
143	0.02	3 Dolomite	0.11	11 Shale	0.01	3 Dolomite	0.02	4 Dolomite
144	0.02	3 Dolomite	0.07	11 Shale	0.01	3 Dolomite	0.02	4 Dolomite
145	0.01	3 Dolomite	0.18	11 Shale	0.03	3 Dolomite	0.02	4 Dolomite
146	0.02	12 Dol.Chert	0.15	11 Shale	0.02	3 Dolomite	0.03	4 Dolomite
147	0.03	3 Dolomite	0.09	11 Shale	0.02	3 Dolomite	0.01	4 Dolomite
148	0.02	3 Dolomite	0.11	11 Shale	0.01	3 Dolomite	0.02	4 Dolomite
149	0.02	3 Dolomite	0.22	11 Shale	0.02	3 Dolomite	0.03	12 Dol.Chert
150	0.03	3 Dolomite	0.20	11 Shale	0.03	3 Dolomite	0.03	12 Dol.Chert

Table II - 2 - 3 (4) Magnetic Susceptibility of Drill Cores

Depth	MJNM-1		MJNM-2			MJNM-3			MJNM-4		
	Mag.sus.	Lithology	Mag.sus.	Lithology		Mag.sus.	Lithology		Mag.sus.	Lithology	
(m)	*1E-3(SI)	No.	*1E-3(SI)	No.		*1E-3(SI)	No.		*1E-3(SI)	No.	
151	0.02	3	Dolomite	0.13	11	Shale					
152	0.03	12	Dol.Chert	0.07	11	Shale					
153	0.02	11	Shale	0.18	11	Shale					
154	0.02	5	Dolomite	0.20	11	Shale					
155	0.02	4	Dolomite	0.13	11	Shale					
156	0.02	4	Dolomite	0.04	11	Shale					
157	0.02	4	Dolomite	0.05	11	Shale					
158	0.02	4	Dolomite	0.01	11	Shale					
159	0.02	4	Dolomite	0.04	11	Shale					
160	0.02	3	Dolomite	0.04	11	Shale					
161	0.02	3	Dolomite	0.02	11	Shale					
162	0.03	3	Dolomite	0.01	11	Shale					
163	0.02	3	Dolomite	0.02	11	Shale					
164	0.03	3	Dolomite	0.02	11	Shale					
165	0.02	3	Dolomite	0.01	11	Shale					
166	0.02	3	Dolomite	0.02	11	Shale					
167	0.02	3	Dolomite	0.01	11	Shale					
168	0.02	3	Dolomite	0.04	11	Shale					
169	0.02	3	Dolomite	0.02	11	Shale					
170	0.05	3	Dolomite	0.02	11	Shale					
171	0.01	3	Dolomite	0.04	11	Shale					
172	0.02	3	Dolomite	0.05	11	Shale					
173	0.02	3	Dolomite	0.07	11	Shale					
174	0.02	3	Dolomite	0.02	11	Shale					
175	0.02	3	Dolomite	0.02	11	Shale					
176	0.02	3	Dolomite	0.01	11	Shale					
177	0.02	3	Dolomite	0.05	11	Shale					
178	0.02	3	Dolomite	0.09	11	Shale					
179	0.02	3	Dolomite	0.04	11	Shale					
180	0.02	3	Dolomite	0.02	11	Shale					
181	0.02	3	Dolomite	0.05	11	Shale					
182	0.02	3	Dolomite	0.16	11	Shale					
183	0.02	3	Dolomite	0.16	11	Shale					
184	0.01	3	Dolomite	0.18	11	Shale					
185	0.02	3	Dolomite	0.15	11	Shale					
186	0.04	3	Dolomite	0.16	11	Shale					
187	0.02	3	Dolomite	0.18	11	Shale					
188	0.01	3	Dolomite	0.13	11	Shale					
189	0.01	3	Dolomite	0.05	11	Shale					
190	0.01	3	Dolomite	0.05	11	Shale					
191	0.02	3	Dolomite	0.04	11	Shale					
192	0.01	3	Dolomite	0.05	11	Shale					
193	0.02	3	Dolomite	0.04	12	Dol.Chert					
194	0.02	3	Dolomite	0.01	12	Dol.Chert					
195	0.02	3	Dolomite	0.02	10	Chert					
196	0.02	3	Dolomite	0.02	10	Chert					
197	0.01	3	Dolomite	0.01	10	Chert					
198	0.01	3	Dolomite	0.04	11	Shale					
199	0.02	3	Dolomite	0.07	11	Shale					
200	0.02	3	Dolomite	0.05	11	Shale					

Table II - 2 - 3 (5) Magnetic Susceptibility of Drill Cores

Depth	MJNM-1			MJNM-2			MJNM-3			MJNM-4		
	Mag.sus.		Lithology	Mag.sus.		Lithology	Mag.sus.		Lithology	Mag.sus.		Lithology
(m)	*1E-3(SI)	No.		*1E-3(SI)	No.		*1E-3(SI)	No.		*1E-3(SI)	No.	
201	0.02	3	Dolomite	0.04	12	Dol.Chert						
202	0.01	3	Dolomite	0.05	12	Dol.Chert						
203	0.02	3	Dolomite	0.02	12	Dol.Chert						
204	0.02	3	Dolomite	0.02	12	Dol.Chert						
205	0.02	3	Dolomite	0.02	5	Dolomite						
206	0.02	3	Dolomite	0.05	5	Dolomite						
207	0.02	3	Dolomite	0.05	5	Dolomite						
208	0.04	3	Dolomite	0.05	5	Dolomite						
209	0.02	3	Dolomite	0.05	5	Dolomite						
210	0.01	12	Dol.Chert	0.02	14	Shale/Sand						
211	0.01	13	Mineraliza.	0.02	5	Dolomite						
212	0.02	13	Mineraliza.	0.01	5	Dolomite						
213	0.02	13	Mineraliza.	0.04	5	Dolomite						
214	0.04	8	Dolomite	0.04	5	Dolomite						
215	0.02	8	Dolomite	0.05	5	Dolomite						
216	0.04	8	Dolomite	0.07	5	Dolomite						
217	0.02	8	Dolomite	0.07	5	Dolomite						
218	0.02	8	Dolomite	0.02	5	Dolomite						
219	0.02	8	Dolomite	0.11	17	Conglo.						
220	0.01	8	Dolomite	0.09	3	Dolomite						
221	0.01	8	Dolomite	0.09	3	Dolomite						
222	0.02	13	Mineraliza.	0.09	3	Dolomite						
223	0.01	13	Mineraliza.	0.04	3	Dolomite						
224	0.01	13	Mineraliza.	0.09	3	Dolomite						
225	0.02	8	Dolomite	0.09	3	Dolomite						
226	0.02	8	Dolomite	0.09	3	Dolomite						
227	0.01	8	Dolomite	0.09	18	Clay min.						
228	0.02	8	Dolomite	0.05	15	Sandstone						
229	0.02	8	Dolomite	0.04	15	Sandstone						
230	0.02	8	Dolomite	0.07	15	Sandstone						
231	0.01	8	Dolomite	0.05	15	Sandstone						
232	0.02	8	Dolomite	0.07	15	Sandstone						
233	0.02	8	Dolomite	0.04	15	Sandstone						
234	0.02	8	Dolomite	0.02	15	Sandstone						
235	0.01	8	Dolomite	0.05	15	Sandstone						
236	0.02	8	Dolomite	0.05	5	Dolomite						
237	0.01	8	Dolomite	0.04	5	Dolomite						
238	0.01	8	Dolomite	0.02	5	Dolomite						
239	0.02	8	Dolomite	0.01	5	Dolomite						
240	0.02	4	Dolomite	0.01	5	Dolomite						
241	0.02	4	Dolomite	0.01	5	Dolomite						
242	0.02	4	Dolomite	0.01	5	Dolomite						
243	0.02	13	Mineraliza.	0.04	5	Dolomite						
244	0.02	4	Dolomite	0.05	5	Dolomite						
245	0.02	13	Mineraliza.	0.02	5	Dolomite						
246	0.02	13	Mineraliza.	0.04	5	Dolomite						
247	0.02	4	Dolomite	0.05	3	Dolomite						
248	0.02	4	Dolomite	0.05	3	Dolomite						
249	0.02	4	Dolomite	0.11	3	Dolomite						
250	0.01	12	Dol.Chert	0.13	3	Dolomite						

Table II - 2 - 3 (6) Magnetic Susceptibility of Drill Cores

Depth (m)	MJNM-1 Mag.sus. *1E-3(SI)	MJNM-1 Lithology No.	MJNM-2 Mag.sus. *1E-3(SI)	MJNM-2 Lithology No.		MJNM-3 Mag.sus. *1E-3(SI)	MJNM-3 Lithology No.		MJNM-4 Mag.sus. *1E-3(SI)	MJNM-4 Lithology No.	
251	0.02	3	Dolomite	0.09	3	Dolomite					
252	0.02	3	Dolomite	0.07	3	Dolomite					
253	0.02	3	Dolomite	0.13	3	Dolomite					
254	0.02	3	Dolomite	0.11	3	Dolomite					
255	0.01	3	Dolomite	0.09	3	Dolomite					
256	0.02	3	Dolomite	0.09	3	Dolomite					
257	0.02	3	Dolomite	0.09	5	Dolomite					
258	0.02	3	Dolomite	0.04	5	Dolomite					
259	0.02	3	Dolomite	0.04	5	Dolomite					
260	0.02	3	Dolomite	0.05	5	Dolomite					
261	0.02	3	Dolomite	0.02	5	Dolomite					
262	0.02	3	Dolomite	0.07	5	Dolomite					
263	0.02	3	Dolomite	0.01	5	Dolomite					
264	0.02	3	Dolomite	0.04	12	Dol.Chert					
265	0.01	12	Dol.Chert	0.01	3	Dolomite					
266	0.01	3	Dolomite	0.02	3	Dolomite					
267	0.02	3	Dolomite	0.02	3	Dolomite					
268	0.02	3	Dolomite	0.04	3	Dolomite					
269	0.01	3	Dolomite	0.02	3	Dolomite					
270	0.02	3	Dolomite	0.04	3	Dolomite					
271	0.02	13	Mineraliza.	0.04	3	Dolomite					
272	0.01	3	Dolomite								
273	0.02	3	Dolomite	0.02	3	Dolomite					
274	0.01	13	Mineraliza.	0.02	3	Dolomite					
275	0.02	12	Dol.Chert	0.04	3	Dolomite					
276	0.01	3	Dolomite	0.01	3	Dolomite					
277	0.02	12	Dol.Chert	0.02	3	Dolomite					
278	0.02	3	Dolomite	0.02	3	Dolomite					
279	0.01	3	Dolomite	0.01	3	Dolomite					
280	0.02	12	Dol.Chert	0.01	3	Dolomite					
281	0.02	3	Dolomite	0.01	3	Dolomite					
282	0.02	13	Mineraliza.	0.01	3	Dolomite					
283	0.02	3	Dolomite	0.01	3	Dolomite					
284	0.01	13	Mineraliza.	0.01	3	Dolomite					
285	0.02	3	Dolomite	0.02	12	Dol.Chert					
286	0.01	3	Dolomite	0.02	12	Dol.Chert					
287	0.01	3	Dolomite	0.01	3	Dolomite					
288	0.02	3	Dolomite	0.01	3	Dolomite					
289	0.04	3	Dolomite	0.01	3	Dolomite					
290	0.01	3	Dolomite								
291	0.02	3	Dolomite								
292	0.01	3	Dolomite	0.01	3	Dolomite					
293	0.01	3	Dolomite	0.07	3	Dolomite					
294	0.01	3	Dolomite	0.01	3	Dolomite					
295	0.01	4	Dolomite	0.02	5	Dolomite					
296	0.01	4	Dolomite	0.01	5	Dolomite					
297	0.01	4	Dolomite	0.07	5	Dolomite					
298	0.02	4	Dolomite	0.11	5	Dolomite					
299	0.01	12	Dol.Chert	0.11	5	Dolomite					
300	0.01	4	Dolomite	0.07	3	Dolomite					

Table II - 2 - 4 Acquired Values of Resistivity and IP of Samples

Sample No.	Depth m	Rock,Mineral name	Electric property											
			Resistivity Ω·m	IP property										
				M=4	5	6	7	8	9	10	11	12	13	14
MJNM1-1	1.10	Calcrete	989.22	0.68	0.58	0.57	0.53	0.42	0.45	0.43	0.38	0.30	0.22	0.15
MJNM1-2	20.00	Calcrete	2322.10	2.31	1.99	1.16	0.83	0.58	0.41	0.34	0.27	0.24	0.24	0.25
MJNM1-3	40.00	Sandy Calcrete	247.18	3.49	3.26	2.88	2.44	2.06	1.64	1.16	0.84	0.50	0.21	0.10
MJNM1-4	61.00	Coarse pebbles	288.90	20.04	18.20	16.14	13.87	11.68	9.36	7.34	5.75	4.40	3.35	2.49
MJNM1-5	78.90	Coarse pebbles	389.80	3.02	2.28	1.94	2.15	2.12	1.78	1.34	0.90	0.52	0.21	0.14
MJNM1-6	99.90	Grainite	423.04	5.49	4.21	3.28	2.51	1.93	1.51	1.22	1.01	0.86	0.73	0.64
MJNM1-7	111.58	Sphalerite Galena disseminated	9439.72	12.93	11.25	9.79	8.34	7.07	5.93	4.95	4.13	3.33	2.70	2.12
MJNM1-8-1	112.30	Galena ore	10597.90	76.43	67.11	58.89	50.90	43.70	37.23	31.63	26.70	22.46	18.78	15.65
MJNM1-8-2	112.30	Galena ore	14895.88	2.05	1.45	1.10	0.83	0.63	0.47	0.38	0.28	0.22	0.18	0.14
MJNM1-8-3	112.30	Galena ore	6279.21	18.25	15.59	13.40	11.37	9.58	8.03	6.74	5.61	4.66	3.88	3.21
MJNM1-9	120.05	Dolomite (well bedded)	858.73	5.64	4.55	3.79	3.12	2.58	2.13	1.79	1.50	1.26	1.06	0.89
MJNM1-10	139.65	Grey dolomite (sandy)	2490.98	2.28	1.57	1.64	1.64	0.61	0.55	0.47	0.38	0.29	0.21	0.15
MJNM1-11	160.00	Dolomite (Massive)	1088.97	10.05	8.31	6.96	5.68	4.59	3.67	2.91	2.31	1.82	1.42	1.12
MJNM1-12	180.16	Dolomite (Massive)	1452.62	5.09	4.12	3.45	2.84	2.33	1.92	1.59	1.32	1.10	0.92	0.76
MJNM1-13	200.00	Dolomite (Massive)	908.33	1.45	0.69	0.72	0.69	0.63	0.54	0.45	0.34	0.25	0.17	0.10
MJNM1-15	220.00	Dolomite (Stylolite dev.)	1535.28	2.04	1.48	1.38	1.30	0.93	0.60	0.35	0.29	0.23	0.17	0.11
MJNM1-16	239.80	Dolomite (Stylolite dev.)	1553.93	2.15	1.54	0.98	0.74	0.73	0.68	0.59	0.49	0.39	0.31	0.22
MJNM1-17	259.90	Dolomite (Massive)	1596.87	1.34	1.10	0.89	0.78	0.42	0.41	0.37	0.32	0.25	0.19	0.13
MJNM1-18-1	245.75	Sphalerite pod	626.70	42.52	38.43	34.73	30.95	27.37	23.98	20.91	18.08	15.57	13.30	11.31
MJNM1-18-2	245.75	Sphalerite pod	459.54	4.34	3.48	2.90	2.39	1.94	1.60	1.34	1.10	0.95	0.80	0.67
MJNM1-18-3	245.75	Sphalerite pod	661.92	2.43	2.06	2.09	1.18	1.22	1.22	1.20	0.17	0.12	0.07	0.03
MJNM1-19	279.00	Dolomite (Massive)	1503.24	1.43	1.07	0.96	0.87	0.83	0.76	0.66	0.54	0.43	0.33	0.24
MJNM1-20	299.90	Dolomite (well bedded)	1545.36	2.04	1.46	1.31	0.98	0.68	0.63	0.57	0.47	0.38	0.29	0.21
MJNM2-1	3.00	Calcrete (brecciated)	960.51	4.31	3.62	3.58	3.41	3.10	2.69	2.25	1.79	1.36	0.97	0.66
MJNM2-2	30.25	Calcrete	1800.36	9.58	8.10	6.97	5.96	5.00	4.25	3.55	2.99	2.50	2.11	1.78
MJNM2-3	60.70	Calcrete (brecciated)	2380.66	10.57	9.01	7.83	6.59	5.43	4.71	4.06	3.32	2.89	2.35	2.00
MJNM2-4	81.00	Dolomite	14646.26	8.43	6.82	5.57	4.44	3.50	2.74	2.13	1.68	1.33	1.04	0.83
MJNM2-5	99.90	Dark grey dolomite	8157.66	4.88	3.92	3.28	2.73	2.23	1.86	1.56	1.32	1.16	0.93	0.78
MJNM2-6	115.00	Black dolomitic shale	24826.55	1.01	0.97	0.85	0.69	0.60	0.60	0.53	0.43	0.35	0.29	0.21
MJNM2-7	151.00	Black dolomitic shale	804.63	8.70	6.75	5.36	4.24	3.38	2.68	2.14	1.72	1.37	1.10	0.87
MJNM2-8	185.00	Shale & Dolomite	243.89	17.90	14.10	11.03	8.40	6.40	4.93	3.85	3.03	2.42	1.89	1.50
MJNM2-9	195.10	Oolitic chert	26726.17	1.73	1.49	1.21	1.01	0.61	0.37	0.28	0.18	0.15	0.10	0.07
MJNM2-10	227.70	Sandstone	17568.51	1.53	0.95	0.68	0.51	0.33	0.24	0.19	0.15	0.13	0.13	0.11
MJNM2-11	251.15	Dolomite	12045.42	6.78	5.42	4.44	3.57	2.91	2.35	1.92	1.56	1.28	1.05	0.87
MJNM2-12	272.33	Massive dolomite	19754.93	5.64	4.57	3.78	3.09	2.50	2.03	1.65	1.35	1.10	0.90	0.73
MJNM2-13	298.40	Massive dolomite	5532.94	16.94	14.19	11.95	9.94	8.19	6.70	5.46	4.42	3.56	2.86	2.28
MJNM3-1	4.00	Calcrete	1232.13	12.24	10.46	8.98	7.59	6.37	5.26	4.37	3.59	2.93	2.41	1.86
MJNM3-2	29.80	Massive dolomite	38567.28	2.48	1.86	1.42	1.04	0.78	0.60	0.55	0.36	0.34	0.28	0.19
MJNM3-3	60.00	Massive dolomite	2289.04	3.56	2.72	2.18	1.73	1.34	1.10	0.90	0.72	0.63	0.53	0.46
MJNM3-4	75.52	Calcareous sandstone	500.03	0.86	0.51	0.30	0.27	0.13	0.08	0.07	0.06	0.11	0.08	0.07
MJNM3-5	91.05	Dolomite	4082.28	1.15	0.74	0.59	0.43	0.47	0.23	0.18	0.15	0.14	0.14	0.14
MJNM3-6	119.75	Dolomite	37987.64	12.72	10.64	9.01	7.57	6.33	5.27	4.40	3.63	3.00	2.48	2.05
MJNM3-7	149.20	Med. - fine dolomite	26039.26	1.19	0.76	0.56	0.40	0.29	0.20	0.14	0.12	0.11	0.09	0.08
MJNM4-1	9.50	Dark grey dolomite	24721.20	1.35	0.87	0.62	0.43	0.30	0.21	0.14	0.11	0.10	0.08	0.08
MJNM4-2	30.80	Grey fine dolomite	25175.09	2.54	1.89	1.50	1.19	0.92	0.71	0.57	0.45	0.39	0.31	0.25
MJNM4-3	60.70	Black sandy shale	7653.76	7.54	6.18	5.12	4.17	3.43	2.78	2.27	1.83	1.51	1.22	1.00
MJNM4-4	94.00	Cream limestone	3359.60	21.51	18.03	15.25	12.66	10.45	8.54	6.99	5.69	4.68	3.75	2.99
MJNM4-5	119.40	Druse dolomite	3797.04	22.72	19.17	16.26	13.57	11.25	9.24	7.63	6.26	5.11	4.16	3.42
MJNM4-6	149.90	Dolomite with sericite layer	1793.40	4.74	3.37	2.44	1.80	1.33	1.02	0.93	0.79	0.76	0.70	0.68

Table II - 2 - 5 Mean Values of Magnetic Susceptibility by Drill Hole and Lithofacies

Magnetic susceptibility average (geometric mean)									
Rock name with Lithological description	litho. num.	MJNM-1 Average *10E-3SI	sum	MJNM-2 Average *10E-3SI	sum	MJNM-3 Average *10E-3SI	sum	MJNM-4 Average *10E-3SI	sum
Calcrete (Less stratified)	1	0.046	42	0.020	16	0.039	9		
Calcrete (Gravel brecci.)	2	0.100	43	0.030	44			0.018	1
Dolomite (Massive)	3	0.017	119	0.022	81	0.017	120	0.025	65
Dolomite (Well bedded)	4	0.014	29			0.049	1	0.019	30
Dolomite (Sandy)	5	0.019	13	0.031	36	0.015	9	0.023	8
Dolomite (Stromatolitic)	7					0.037	3		
Dolomite (Stylolite developed)	8	0.016	23						
Chert	10			0.014	3	0.016	1	0.018	1
Shale	11	0.016	4	0.029	95	0.033	2	0.023	12
Chart&Dolomite	12	0.014	9	0.023	10			0.033	2
Mineralization	13	0.015	18						
Shale//Sandstone	14			0.018	1				
Sandstone	15			0.046	8	0.016	3		
Shale//Dolomite	16							0.022	3
Conglomerate	17			0.109	1				
Clay mineral zone	18			0.091	1				
Whole drill core		0.024	300	0.027	296	0.018	148	0.023	122

Table II - 2 - 6 Mean Values of Resistivity and IP values by Lithofacies

Drill core resistivity & I.P. value average (geometric mean)				
Rock name with Lithological description	litho. num.	sum	Resistivity Ω・m	IP(M12) mV/V
Calcrete (Less stratified)	1	4	1,502	0.85
Calcrete (Gravel brecci.)	2	5	576	1.35
Dolomite (Massive)	3	17	6,033	0.75
Dolomite (Well bedded)	4	4	2,770	0.44
Dolomite (Sandy)	5	2	1,027	0.50
Dolomite (Stylolite developed)	8	2	1,545	0.30
Chert	10	1	26,726	0.15
Shale	11	4	2,471	1.15
Mineralization(Pod,Veinlets)	13	7	2,914	2.02
Sandstone	15	2	2,964	0.12
Limestone	19	1	3,360	4.68

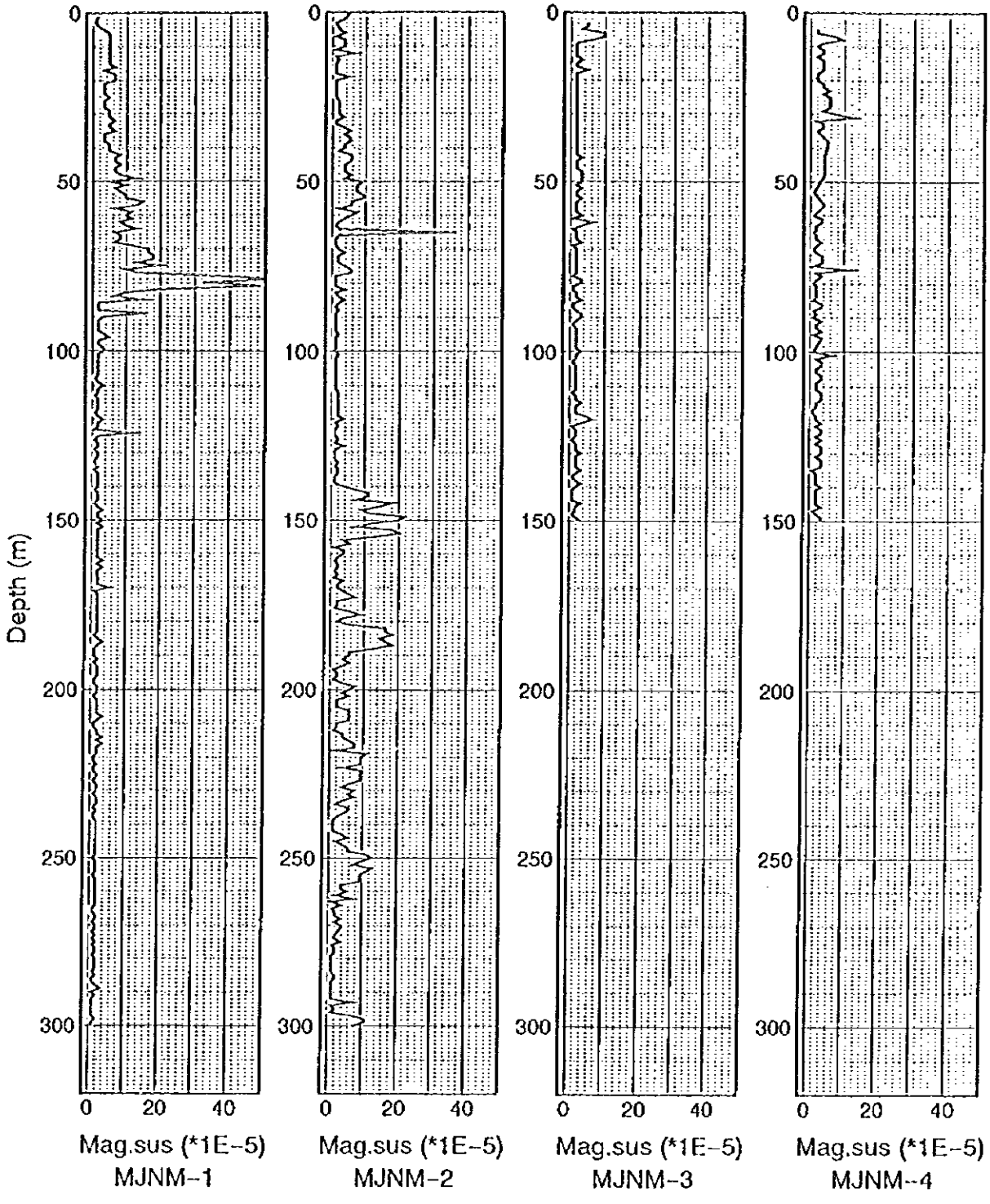

Fig. II - 2 - 1 Magnetic susceptibility distribution of drill holes

Table II - 2 - 7 Electric Conductivity of Ground Water

Location	Observed data				Temperature = 20℃	
	Date	Conductivity mS/cm	Reisitivity Ω・m	Water temp. ℃	Conductivity mS/cm	Reisitivity Ω・m
Near the MJNM-2	11/4/96	1.275	7.84	30.0	1.020	9.80
Max Planck Station	11/4/96	1.014	9.86	28.0	0.852	11.74
Otjikoto Lake	11/4/96	0.970	10.31	28.0	0.815	12.27
Near the MJNM-4	11/4/96	0.974	10.27	26.0	0.857	11.67
Around Abenab	11/4/96	0.960	10.42	28.0	0.806	12.40
Grasvlakte farm	11/10/96	1.270	7.87	36.4	0.853	11.72
Tamboti park	11/10/96	1.100	9.09	29.5	0.891	11.22
Guinab farm	11/11/96	1.113	8.98	26.9	0.959	10.42
Average					0.882	11.41

II-2-3-2. Interpretation of resistivity and chargeability data

(1) Resistivity of rock

The materials such as rocks constituting the earth crust are essentially insulators when no moisture is included, except for graphite. Consequently the resistivity of those materials depend mainly upon interstitial water saturation, water distribution and water resistivity. The higher water saturation the soil and rock may have, the smaller resistivity they may have.

On the other hand, the resistivity grows rapidly with the lower resistivity. The more electrolyte the pore water dissolves, the lower resistivity the water may have. Archie formula indicates the relationship as follows.

$$\rho_s = a\,\rho_w / \phi^m S^n$$

{ ρ_s: resistivity of rock and soil; a : proportion coefficient; ρ_w : water resistivity; ϕ : porosity; S : water saturation rate; m : cementation factor; n : saturation index (=2)}

When a sample contains conductive minerals such as ores the resistivity greatly varies with the mineralogy and the amount. The more a sample contains conductive mineral, the lower resistivity it may have. If the mode is in the order of 5% the resistivity is rarely affected however, when it exceeds 25% the sample would give less than a half of the resistivity of the mineral leading to the remarkable low resistivity in a whole.

When an argillaceous mineral occurs, the Archie formula could not be applied for interpretation. For instance, pelitic rock would not observe the Archie formula and would give much lower values than expected. The larger surficial area an argillaceous mineral has, the larger conductivity it may have because the current conducts along the surface of the mineral depending on excessive ionization in an electric double layer. Further, the specific larger cation exchange capacity(CEC) of an argillaceous mineral, the greater conductivity it may have. For example, the CEC of vermiculite is considerably large resulting in the remarkable low resistivity of the vermiculite bearing soil and weathered product of rock. The argillaceous minerals derived of ultrabasic rock may give lower resistivity than those derived of acid rock. Palacky(1986) refers 2 to 20 Ω・m for the former and 20 to 200 Ω・m for the latter.

The factors controlling the resistivity of rock are important particularly for the interpretation of the airborne geophysical data.

Factors of resistivity of rock and soil

low	resistivity ρ	high
wet	moisture	dry
(pore water resistivity is for control factor)		(the amount of conductive mineral is control factor)
low	resistivity of pore water ρ_w	high
(high ion concentration)		(low ion concentration)
large	porosity(saturation)	small
large	water saturation	small
abundant	abundance in conductive mineral	poor
(important when >25%)		(negligible when <5%)
abundant	argillaceous mineral	poor
large	CEC of argillaceous mineral	small

(2) Principle of IP method

When the current is introduced underground a series of electrochemical phenomena would occur within the constituent particles, of which the following two are detected by IP method.

Over voltage effect : The current introduction gives rise to electric double layer on the sulphide or metallic conductive substance and the current interruption causes discharge to the opposite direction against the introduction. This phenomenon is an effect of combination of ionic conduction with electronic conduction and enables the IP method for such minerals of electronic conductivity effective.

Normal effect or Background : The effect is a varying polarization occurring in the common rock when the current is introduced, being brought chiefly by membrane polarization of the argile included in the pores of a rock in a small quantity. Montmorillonite shows the most intense effect among the clay minerals and kaolinite the weakest. The membrane polarization reaches the maximum value when the volume ratio of clay to rock is as much as 5 percent, as far from which it declines. The maximum value locating close to 5 percent of the montmorillonite ratio is translated approximately 2 percent in terms of FE value and is small enough compared to Over Voltage effect.

The observed IP effect is termed chargeability and is expressed as Vs(tn)/Vp{mV/V}. The polarization ratios of Frequency method and Time domain method give experimental value of 1 percent and 5 mV/V respectively.

(3)Analysis of observed values

The correlation between resistivity and chargeability(IP) was figured from the observed values(Fig.II-2-2). The figure was divided into three resistivity zones and four IP zones using thresholds for interpretation.

Zone	range	characteristics
Resistivity A	less than 300 Ω·m	• massive sulphide and argillaceous minerals • Shale and boulder bearing calcrete • sometimes barrier for interpretation
Resistivity B	300 to 4,000 Ω·m	• disseminated ore minerals and weathered shale • could be favourable target but mostly the result of Phase II falls

		within this zone
Resistivity C	more than 4,000 Ω · m	· fresh massive dolomite · mineralisation of pod-like galena
IP I	no less than 100mV/V	· massive sulphide. · favourable target for mineralisation if the volume is enough · no sample is recognized in this zone
IP II	100 to 10mV/V	· disseminated ore minerals · the most common zone for IP survey · some of the mineralisation fall in this zone
IP III	10 to 1mV/V	· weak dissemination of ore minerals and rock abundant in argillaceous mineral · the mineralisation of core samples · the half number of core samples · pebble bearing calcrete
IP IV	less than 1 mV/V	· dolomite, chert and massive calcrete

II-2-4. Discussion

(1) A core sample mineralised with pod like galena hosted by dolomite revealed high resistivity averaging 10000 Ω · m. The ore mineral itself is believed to have low resistivity). The high resistivity possibly resulted from massive ore surrounded by low resistivity. Although the electromagnetic geophysical survey may not detect sporadic mineralisation as the one located, an electromagnetic survey is capable of detecting low resistivity anomalies within an overall high resistivity area.

(2) Some lithofacies of calcrete show considerably high IP values. The pebble bearing calcrete with low resistivity acts as a barrier for direct current electric ground geophysical surveys.

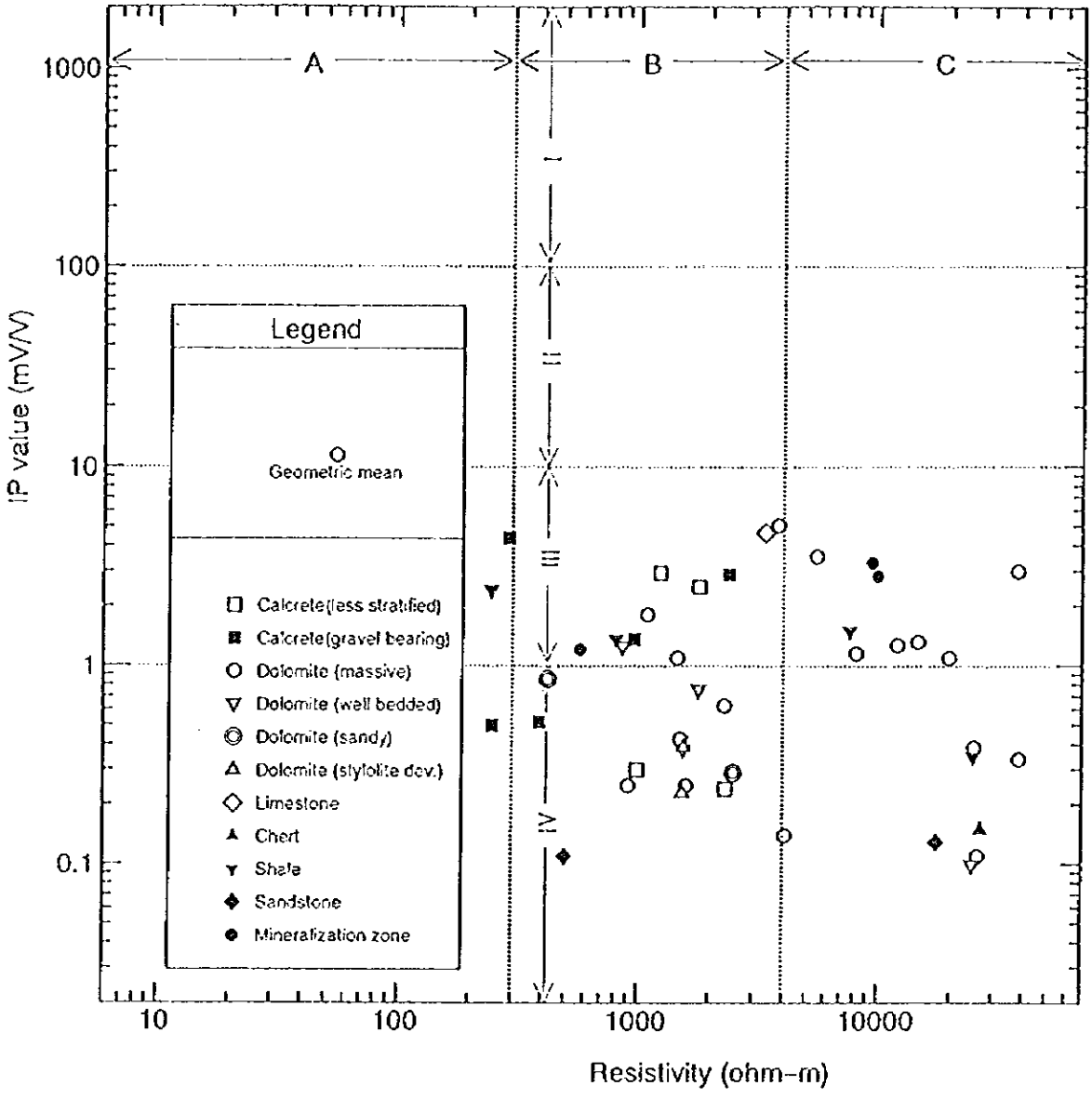

Fig. II - 2 - 2 Core sample resistivity v.s.IP value

Chapter 3 Airborne Geophysical Survey

II-3-1. Objective and Method of AEM

The objective of the survey is to obtain the subsurface resistivity maps and to extract low resistivity anomalies which may derived from sulphide deposits over the survey area where no proterozoic formations expose being covered by calcrete sediment.

The electromagnetic (EM) method is a survey method which uses electromagnetic induction to measure the distribution of resistivity in the Earth as well as to locate buried electrically conductive bodies such as ore deposits. There are various measuring systems for the electromagnetic method. The Dighem V airborne EM system employs the in-phase / quadrature measuring method.

This method uses a combination of transmitter (Tx) coil and receiver (Rx) coil with fixed coil spacing and measures the phase components (in-phase and quadrature components) of the mutual inductance between the coils which vary due to the effect of the Earth's induction. An EM instrument is moved over a survey line to observe the variation of the phase components and the subsurface resistivity distribution below the survey line can be obtained by analyzing the measured data according to the EM theory described later.

Fig.II-3-1 illustrates the concept of electromagnetic-induction in the EM method. The transmitter (Tx) coil generates an alternating primary magnetic field, shown as a solid line. When this passes through a buried conductor, an eddy current flows inside the conductor. The eddy current generates the secondary magnetic field shown by dashed lines in the figure, which is measured by a receiver (Rx) coil.

In order to get a qualitative concept of how a conductor responds to EM equipment, consider a single turn coil having a resistance (R) and a self inductance (L) as a simple model of a conductor. When an alternating current with frequency f [Hz] flows in the Tx-coil, a primary field (Hp) is produced. The induced current within the single turn coil generates the secondary field(Hs). The Rx-coil detects the synthetic field of Hp and Hs.

The ratio of Hs to Hp is given by the following formula (Grant and West, 1967).

$$Hs/Hp = K \cdot \frac{\alpha^2 + j\alpha}{1 + \alpha^2} = K \cdot f(\alpha), \quad \alpha = \omega L / R, \quad \omega = 2\pi f$$

K is a coefficient which includes L as well as the mutual impedances between the three coils and represents the amplitude of EM response. K becomes smaller when the Tx-Rx coil-pair is located far from the single coil, and this means that the EM response becomes smaller when the height of the EM sensor becomes larger.

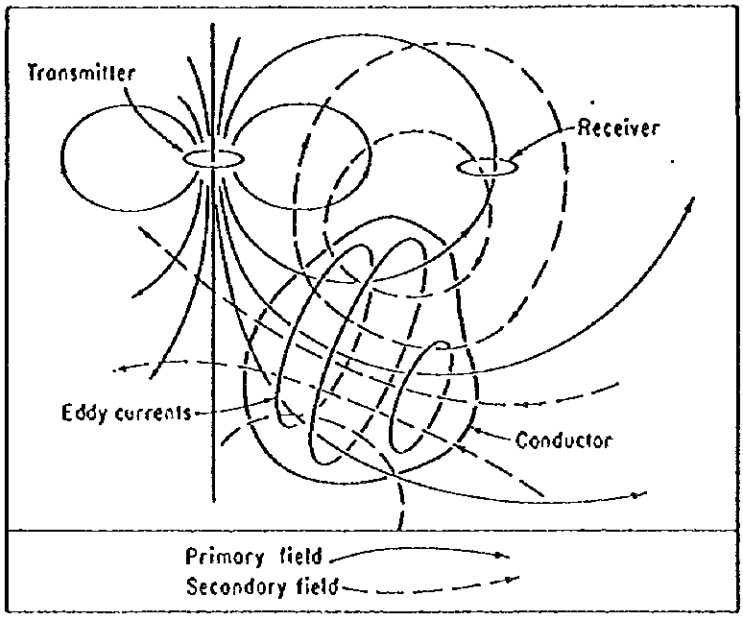

Fig. II - 3 - 1 Concept of EM induction

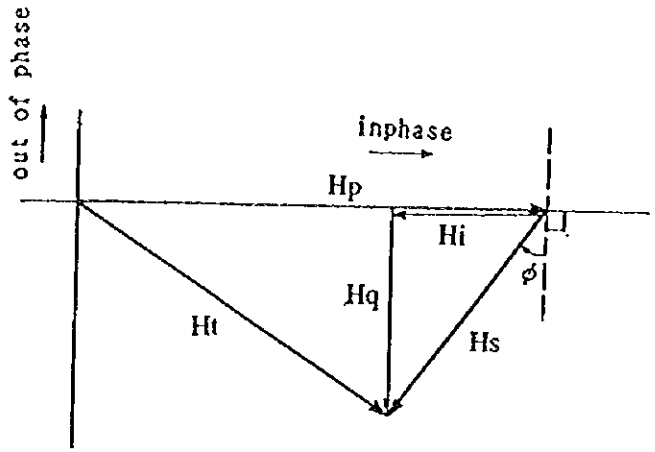

Hp : primary field

Hs : secondary field

Hi : in-phase component of secondary field

Hq : Out-of-phase component of secondary field

Fig. II - 3 - 2 Diagram of phase relationship

f (α) is a complex function called the response function and shows that Hs has both real and imaginary parts. The real part is in-phase to Hp, and the imaginary part is out-of-phase(quadrature) to Hp. The absolute value of f (α) is less than 1 and close to zero when R is high, and close to 1 when R is low, which means that EM response becomes larger when the resistivity of the earth becomes low. Fig.II-3-2 shows the phase relation of Hs and Hp. By measuring both in-phase(Hi) and quadrature(Hq) components simultaneously, α can be calculated, giving the estimates of the electrical property of the single coil.

In the airborne electromagnetic method, the EM equipment is carried aboard an airplane or a helicopter and surveys the distribution of resistivity in the Earth. By towing the EM sensor at a height of 30m to 100m over a survey line, and recording the EM response and analyzing the recorded data, the resistivity map is made. In addition to being called AEM (Airborne ElectroMagnetic prospecting) method, the term HEM (Helicopter-borne ElectroMagnetic method is used.

II-3-2. Survey Specifications and Equipment

II-3-2-1. Specifications

The main specifications are mentioned below.

(1)Location and Coverage

Fig.I-1-1 illustrates the survey area with a coverage of 904 km2 where the data acquisition of resistivity was conducted.

(2)Direction of the flight line is true north to south and the interval is 200 metres with tie lines of 5 km interval. The shortest flight line is 2500m long and the total line kilo is 4895 km.

(3)Air craft

Bell-Long Ranger III ZS-RFA helicopter was used.

(4)Altitude was maintained at 35 m for electromagnetic and 50m for aeromagnetic.

(5)Lateral sampling interval is less than 6 metre.

(6)Navigation was of GPS-Video tracking system

Flight pass map and boundary points of the survey area are shown in Fig.II-3-3 and Table II-3-1 respectively.

Table II－3－1　Boundary Points of the Survey Area

	XTM	YTM	Latitude			Longitude		
			°	′	″	°	′	″
1	131410E	303956S	19	15	00.000S	17	45	00.000E
2	131503E	316871S	19	08	00.000S	17	45	00.000E
3	63118E	317233S	19	08	00.000S	18	24	00.000E
4	63083E	307087S	19	13	30.000S	18	24	00.000E
5	87617E	306986S	19	13	30.000S	18	10	00.000E
6	87579E	299053S	19	17	48.000S	18	10	00.000E
7	105096E	298960S	19	17	48.000S	18	00	00.000E
8	105126E	304126S	19	15	00.000S	18	00	00.000E

II-3-2-2. Equipment

The equipment used in this airborne EM survey is the DIGHEM V system produced by the Canadian firm DIGHEM. Dighem V system consists of a EM unit (EM response measuring unit), a high-sensitivity magnetometer, a radio altimeter, a GPS navigation system, a tracking video camera, and analog- and digital recorders. The specifications of the Dighem V system are shown in Table II-3-2.

Fig.II-3-4 is a diagram of the in-flight measurement. The EM console was loaded on the helicopter. An EM sensor (or EM bird) and a magnetic sensor(or Mag-bird) are towed by a 30m long towing cable. The cable contains multi-conductors and is bundled together with a steel wire. A shear pin has been designed to break so that in case of a sudden shock the bird will fall free of the helicopter.

The EM unit consists of the EM sensor and EM measuring circuits contained in the EM console. The EM bird is a cylinder 10m long and 50cm in diameter made of fiber reinforced plastic containing four pairs of transmitter/receiver coils, and is electrically connected to the EM console through the cable.

Dighem V measures eight channels of EM responses, that is, in-phase and quadrature for each of four frequencies. Both Hi/Hp and Hq/Hp are measured in ppm units, and recorded digitally. Three pairs of horizontal-coplanar coils are suitable for resistivity mapping, and a vertical-coaxial coil-pair is good for detecting steeply dipping conductors. The magnitude of the secondary field(Hs) is much smaller than the primary field(Hp), therefore the EM unit is designed to measure Hs accurately by means of canceling Hp in the circuits.

Table II-3-2 Specifications of Equipment

Item	Manufacturer · Type · Specifications etc.	No
Aircraft (Helicopter)	Bell Long Ranger L3-ZS-RFA	1
Magnetometer	Scintrex H8 cesium vapor optically pumped magnetometer with the sensor installed in a tail stinger pod.	1
Acquisition system	RMS DAS 8 -including: RMS 4183A micro computer module RMS 4185A analogue input module RMS 4239A tape interface module RMS 4272A smart serial interface module RMS 4137 digital interface module RMS TDC 3620 tape cartridge recorder, interfaced to the digital acquisition system via the RMS 4239A module RMS GR33A chart recorder	1
Compensator	RMS AADC II,27 terms.	1
Flight path tracking	National Panasonic AG-7450 S-VHS video system recorded to VHS cassette, in the European PAL format.	1
Navigation & flight path recovery	Two NovAtel 3151R GPS receivers for flight location and base station location information operating in real time differential mode.	1
Altimeter	Sperry 200-A radar linear tracking altimeter	1
Barometer	Intellisensor AIR-DB-2B digital barometer /altimeter	1
Base Magnetometer	Scintrex H8 Cs vapor magnetometer	1
Processing platform	IBM-PC 486 computer with SCSI tape drive	1
Base receiver	NovAtel 3151 GPS receiver employing a PC driven NovAtel GPS card TM Performance 3151R	1

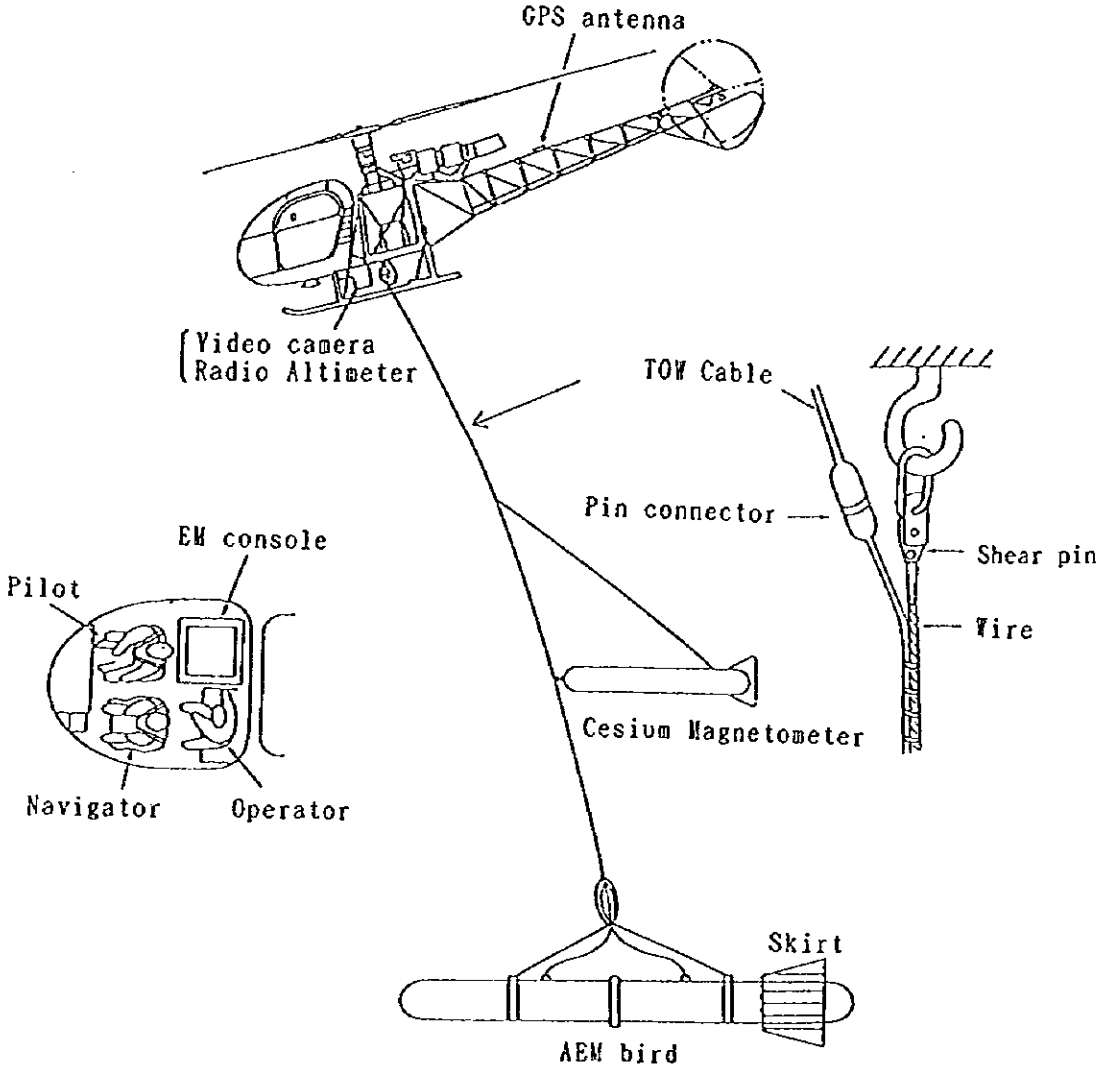

Fig. II - 3 - 4 AEM instruments in use

The magnetometer consists of a magnetic sensor and a measuring unit. The Mag-bird is a cylinder 3m long and 25cm in diameter made of fiber reinforced plastic, containing an optical pumping Cesium magnetometer. The measuring unit is set in the EM console, and the values of total magnetic intensity are recorded digitally.

GPS antenna was attached to the roof of the cabin. A computer for GPS calculation was set in EM console, and the GPS coordinates of the helicopter positions were output into the digital recorder.

The tracking video camera and the radio altimeter were placed on the skid.

The altitude of the helicopter above the ground was measured by the radio altimeter and recorded digitally.

The electric power for these equipments were supplied by the battery of the helicopter.

II-3-3. Data Acquisition

The EM equipment is calibrated on the ground before commencing the survey. After warming up for at least thirty minutes, a 'ferrite bar' is placed in the predetermined position on the side of the receiver coil for adjusting the in-phase and out-of-phase amplitude for each frequency and then the Q coils are set to adjust the amplifier gain for four frequencies.

The automatic recording proton magnetometer is set near the heliport and records the variation of geomagnetic field, which is used for the diurnal correction of measured aeromagnetic field value as well as for monitoring magnetic storms.

The crew of the helicopter are three: a pilot, a system operator and a navigator. After leaving the heliport, each EM reading is reset at 0 level at an altitude more than 300m before commencing the line survey, and also every 15 or 20 minutes during the flight.

The helicopter flies at 60m to 130m above the ground so that the EM bird is kept at 30m to 100m while flying over the survey line. The flight speed depends upon topography; in mountainous areas 30-40km/h is normal, while over flat land 100km/h is normal.

The GPS navigation method was employed principally in this survey, using visual navigation as a supplementary method.

The GPS navigation system measures the present location of the helicopter by receiving information from GPS satellites. An indicator placed in front of the pilot displays the actual flight path as well as the planned flight lines. The coordinate values of the path are recorded every .1 second, and used to make the survey line map later.

For visual navigation, planned flight lines were drawn on a 1:50,000 topographic map. When the helicopter passes over a landmark, the navigator marks with a fiducial number on the map(fiducial point). The fiducial numbers are continuously displayed on the indicator every 0.1sec and the same number is recorded on the video image. Later, by comparing the fiducials on the topographic map and

the video image, the flight track is confirmed.

The operator has to confirm that the equipment is operating properly by observing the analog monitor recorder and to maintain the quality of the data. Especially, the operator must be careful for the occur of spheric noise and of the drifting of the 0 level in EM records.

After about two hours flight, the helicopter must return to the supply base for fueling. When landing, the persons on the ground must catch the EM bird and Mag-bird in air to prevent shocks to the birds. To prevent drift in the electronic circuits during the twenty to thirty minutes of refueling, the equipment must be left running by an auxiliary power supply prepared in the heliport.

The above cycle is repeated throughout the survey. The flight may be stopped on occasion when poor weather makes helicopter flight difficult or when a high level of spherics results in marked noise in the data. Production summary is shown in Table II-3-3.

II-3-4. Data Processing

II-3-4-1. Data Base

The digital data of EM responses, total magnetic intensity, altitude, and GPS coordinates recorded on magnetic tapes are edited by a computer and stored in the memory in a form of 'data base', which is used later for data processing and analysis.

II-3-4-2. Flight path recovery

The flight path of the helicopter is mapped using the GPS coordinates of the fiducial points. When parts of the GPS information are omitted or erroneous, the path is corrected by comparing the video image with the topographical map.

II-3-4-3. Calculation of Apparent Resistivity

Apparent resistivity (a) is calculated from in-phase (Hi/Hp) and quadrature (Hq/Hp) values according to EM theory as follows.

Since the EM method uses very low frequencies, the displacement current can be ignored. The basic formula which follows from Maxwell's equation is as follows.

Within conductor: $\nabla^2 H = j \mu \omega \sigma H$ (diffusion equation of vector)

Outside of conductor: $\nabla^2 H = 0$ (Laplace's equation),

where H is the magnetic vector, j is an imaginary unit {=SQR(-1)}, is magnetic permeability, and is conductivity.

Formulas for the EM response of a two-layered earth model were introduced from the basic equations as follows (Frischknecht, 1967).

Table II - 3 - 3 Production Summary of Airborne Electromagnetic Survey

Date	Day	Flight No.	LineKm	Comments
19-Sep-96	Thur.			Mobilise from Windhoek to Tsumeb Work on EM bird (frequency change)
20-Sep-96	Fri.			Work on EM bird
21-Sep-96	Sat.			Work on EM bird
22-Sep-96	Sun.			First flight aborted - nav. problems
23-Sep-96	Mon.	1,2,3,4	400	Operations normal
24-Sep-96	Tues.	5	100	Work on EM bird - one flight only
25-Sep-96	Wed.			100 hour inspection
26-Sep-96	Thur.			100 hour inspection
27-Sep-96	Fri.	6,7,8,9	650	Operations normal
28-Sep-96	Sat.	10,11,12	430	Very turbulent
29-Sep-96	Sun.	13,14	265	Cut short due to turbulence
30-Sep-96	Mon.	15a,15b,16	265	Mag spiking & EM noise
1-Oct-96	Tues.	17		Mag console u/s & EM frequency problems
2-Oct-96	Wed.	18	100	Mag u/s, infield frequency change on EM
3-Oct-96	Thur.			Analog input module failed
4-Oct-96	Fri.			Request replacement parts
5-Oct-96	Sat.			Collect parts in Windhoek
6-Oct-96	Sun.			Gearbox mount problem
7-Oct-96	Mon.			Wait for parts to be sent to Windhoek
8-Oct-96	Tues.			Helicopter to Windhoek
9-Oct-96	Wed.			Helicopter repaired and return
10-Oct-96	Thur.	19	150	One flight due to intermittent mag console problem
11-Oct-96	Fri.	20,21,22	504	Operations normal
12-Oct-96	Sat.	23,24,25,26,27	556	Operations normal
13-Oct-96	Sun.	28,29,30	420	Operations normal - spherics in pm
14-Oct-96	Mon.	31,32,33	337	Operations normal, late start due to GPS batteries low - replaced
15-Oct-96	Tues.	34,35,36	337	Operations normal
16-Oct-96	Wed.	37,38,39	275	Operations normal
17-Oct-96	Thur.			Final processing & packing
18-Oct-96	Fri.			Demobilise

Horizontal-coplanar coil-pair: $(Hs/Hp)_H = B^3 T_H$

Vertical-coaxial coil-pair: $(Hs/Hp)_V = B^2 (T_V - B T_H) / 2$

where,

$$T_H(A, B) = \int_0^\infty R(D, g)\, g^2 e^{-gA} J_0(gB)\, dg$$

$$T_V(A, B) = \int_0^\infty R(D, g)\, g^2 e^{-gA} J_1(gB)\, dg$$

$$R(D, g) = 1 - 2g \frac{\{(U+V) + (U-V) e^{-UD}\}}{(U+g)(U+V) - (U-g)(U-V) e^{-UD}}$$

$$U = (g^2 + 2j)^{1/2}$$

$$V = (g^2 + 2jk)^{1/2}$$

J_0 : 0 Field Bessel Function

J_1 : Primary Field Bessel Function

g : a constant of integration

$$\delta = \left[\frac{2}{\rho_1 \mu \omega} \right]^{1/2}$$ (μ : magnetic permeability), $\omega = 2\pi f$.

$k = 1/2$

$A = 2h/$ *(h : height of bird)

$B = s/$ *(s : separation between transmitter and receiver coils)

$D = 2d/$ *(d : thickness of first layer)

In order to calculate an apparent resistivity, a set of 'phasor diagrams' are prepared. The phasor diagram is an interpretive diagram which shows the relation between the amplitudes of in-phase(Hi) and quadrature(Hq) components and two parameters, i.e., the resistivity (ρ) of homogeneous earth and the bird height (h). Taking Hi as the abscissa and Hq as the ordinate on a complex plane, two sets of curves are drawn corresponding to the two parameters.

Fig.II-3-5 is an example of phasor diagram prepared for a Tx-Rx coil-pair which has a horizontal-coplanar array, coil spacing = 8.0m, and frequency = 900Hz. The apparent resistivity (ρ_a) and the

apparent height of sensor (h_s) can be read on the phasor diagram by plotting the values of the Hi and Hq components. It can be seen that the response decreases with higher altitude, and the ratio Hi/Hq becomes larger when the resistivity becomes lower.

Four sheets of phasor diagrams are prepared for each of DIGHEM's four coil-pairs, and the apparent resistivity is calculated for each of four frequencies.

The computer software for Dighem system contains the equivalent algorithm to the phasor diagrams. By inputting the in-phase and out-of-phase data from the database, the apparent resistivity ρ_a ($\Omega \cdot m$) and apparent height of the EM sensor (m) are output.

II-3-4-4. Resistivity Mapping

Apparent resistivity maps were produced for three frequencies: 900Hz, 7200Hz, and 560000Hz, using the apparent resistivity values that were calculated by the above-mentioned method. A color plotter was used for drafting the maps.

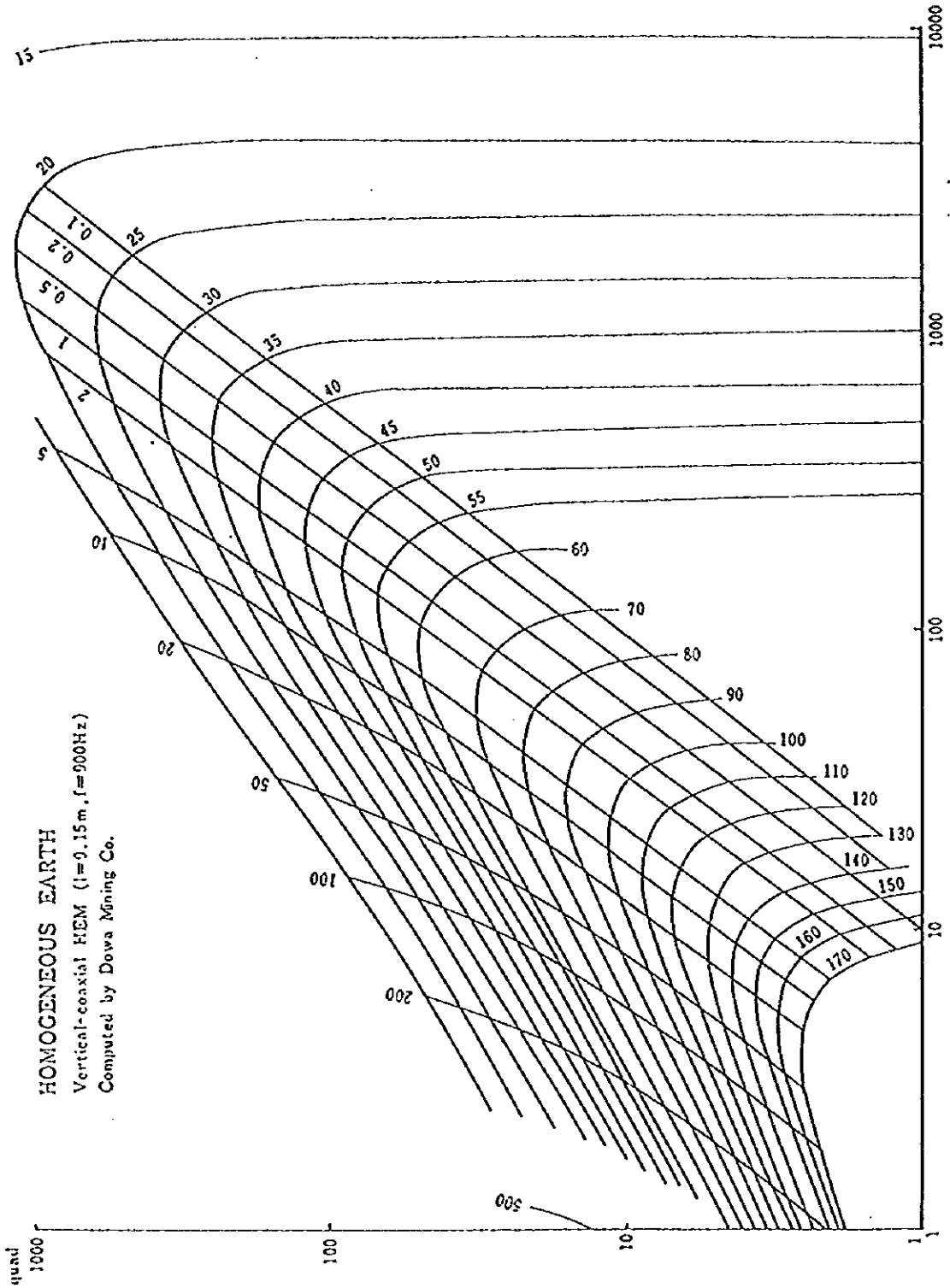

Fig. II - 3 - 5 Phasor diagram

II-3-5. Result and Interpretation

The results are presented as apparent resistivity maps using three frequencies in a coplanar coil deposition (Fig.II-3-7 to Fig.II-3-12), and an apparent resistivity cross sections (Fig.II-3-13) using the differential resistivity versus depth calculation method (Huang et Fraser 1996). Processed Electromagnetic image maps with the emphasis on resistivity lineaments are shown in Fig.II-3-10 to Fig.II-3-12. For reference purposes, the same index as used during the compilation and interpretation of Phase I was adopted.

II-3-5-1. Interpretation for resistivity map 56000Hz (Fig.II-3-7, Fig.II-3-10)

(1) Of the three frequencies analyzed, the resistivity of 56000Hz shows the shallowest structures. Although the detecting depth may vary with the ground resistivity, the 56000Hz frequency is effective from about 100 metre depth in the high resistivity zone which is equivalent to 10000 Ω・m to10 metre depth in the low resistivity zone of 100 Ω・m.

(2) The three resistivity maps are comparable to the existing geological maps and the aeromagnetic anomaly maps. In blocks A through D, four subparallel fold axes of an east-west trend forming a syncline and anticline are traced. In blocks A and B these axes plunge easterly while in the block D4 they plunge westerly. The low resistivity band meandering along the fringes of the synclinorium is correlated to a pelitic or psammitic layer of the upper Tsumeb subgroup. The inner bands of high resistivity and broad low resistivity in the inner direction may coincide with contact of the uppermost dolomite of the Tsumeb subgroup and Mulden group. The Tsumeb subgroup/Mulden group contact coincides with that delineated by the aeromagnetic lineaments.

(3) In block B, the resistivity of the subsurface Mulden group is lower in the south than in the north, suggesting that the calcrete with high resistivity is thin or lacking.

(4) In the east of the survey area the resistivity is generally high except in block E4 which includes an area of low resistivity. The contact between the low and high resistivity coincides with an fault located by the aeromagnetic survey. This fault cuts the Tsumeb subgroup and the basement complex.

(5) An isolated low resistivity zone is delineated over an area of 2 km by 500 m within the overall high resistivity terrain. The zone is extends subparallel to the fold axis and is correlated to the upper Tsumeb subgroup. It is interpreted to reflect an area of local low resistivity. This zone has uniform resistivity values for the three frequencies in the order of 50 to 100 Ω・m, indicating that the zone may extend to a depth of 150 m or more.

(6) With the 56000Hz frequency, the low resistivity zone situated over the A2/A3 boundary is the most remarkable. In the two other frequencies the zone reduces and shows higher resistivity. It is therefore interpreted as resulting from a shallow-seated weathered rock or alternately an aquifer. The

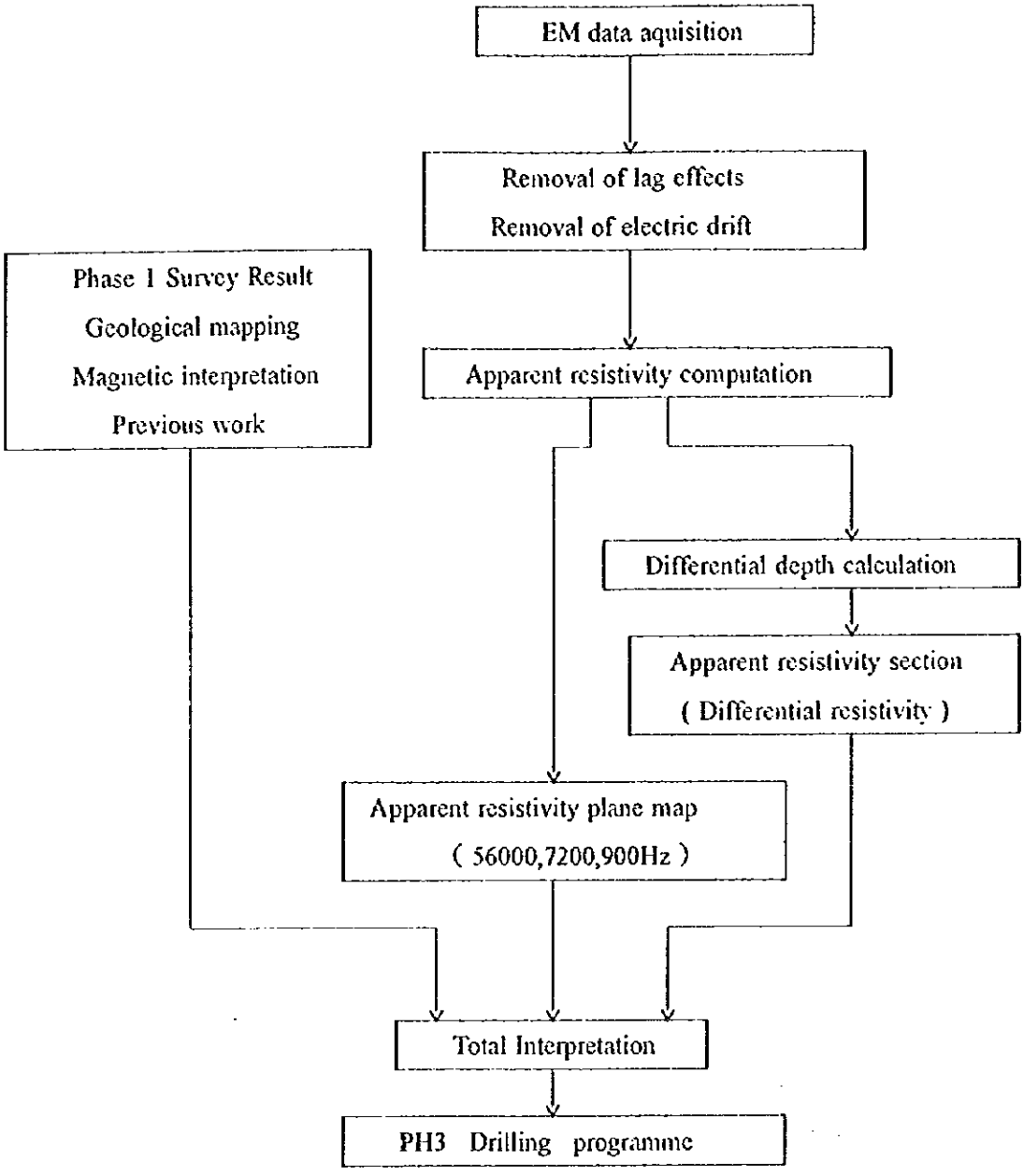

Fig. II - 3 - 6 Flow chart of the electromagnetic survey

resistivity values vary from 50 Ω・m near surface to 150 Ω・m at 50 m deep to some hundreds Ω・m at greater depth.

II-3-5-2. Interpretation for resistivity map, 7200Hz (Fig.II-3-8, Fig.II-3-11)

(1) The general trend of the resistivity for this frequency is similar to that of 56000Hz with general lower resistivity than the latter. The target depth is 300 m in the high resistivity terrain of 8000 Ω・m and 50 m in the low resistivity terrain of 100 Ω・m.

(2) The low resistivity band of the upper Tsumeb subgroup mentioned in II-3-5-2(2) deepens further, and another low zone related to the Mulden group gives slightly higher resistivity than those of 56000Hz. This is attributed to the upper Tsumeb group extending deeper and the Mulden group being significantly thinner or alternately the surficial layer produces lower resistivity due to weathering.

(3) The Mulden group in blocks B2 and B3 shows lower resistivity than in the 56000Hz frequency.

(4) The low resistivity band of the upper Tsumeb can be traced from blocks E3 towards H3. In G3 and H3 a low resistivity zone is recognized which may suggest that the synclinal Mulden group is plunging to the west.

(5) The basement complex which occurs in the southeast of the survey area as indicated by aeromagnetic survey, gives pervasive low resistivity. This is believed to be due to the presence of the argillaceous mineral (saplorite) which forms through weathering of ultrabasic rock.

The cross section indicates that the low resistivity layer may be some 50 metre thick and this is underlain by unaltered basement with high resistivity.

(6) In blocks H2 and H3, a low resistivity lineament trends northwesterly. No lineaments are present in the 56000Hz map but a significantly remarkable lineament is traced in the 900 Hz map suggesting that the lineament may extend to depth. The lineament cuts sedimentary structures and where it cuts the fold axis, the resistivity is reduced even more. Bore hole MJNM-1 is situated at the tip of low resistivity branch originating from the lineament. In addition, parallel to the lineament a resistivity limit is recognized in blocks G2 and G3. A low resistivity zone extends to the east of the limit and may indicate alteration and an independent structural domain. The limit is parallel to the aeromagnetic lineaments which are correlated to the western limit of the dolerite dykes swarm.

(7) The low resistivity zone mentioned in II-3-5-2(6) is also evident in this map and some spots of low resistivity coincide with the northeast trending aeromagnetic lineaments attributed to the dolerite dykes. This trend, which is also evident on the 900 Hz map, can be due to partial altered dolerite or mineralisation. However, the topographic map suggests that it could also be caused by artificial structures.

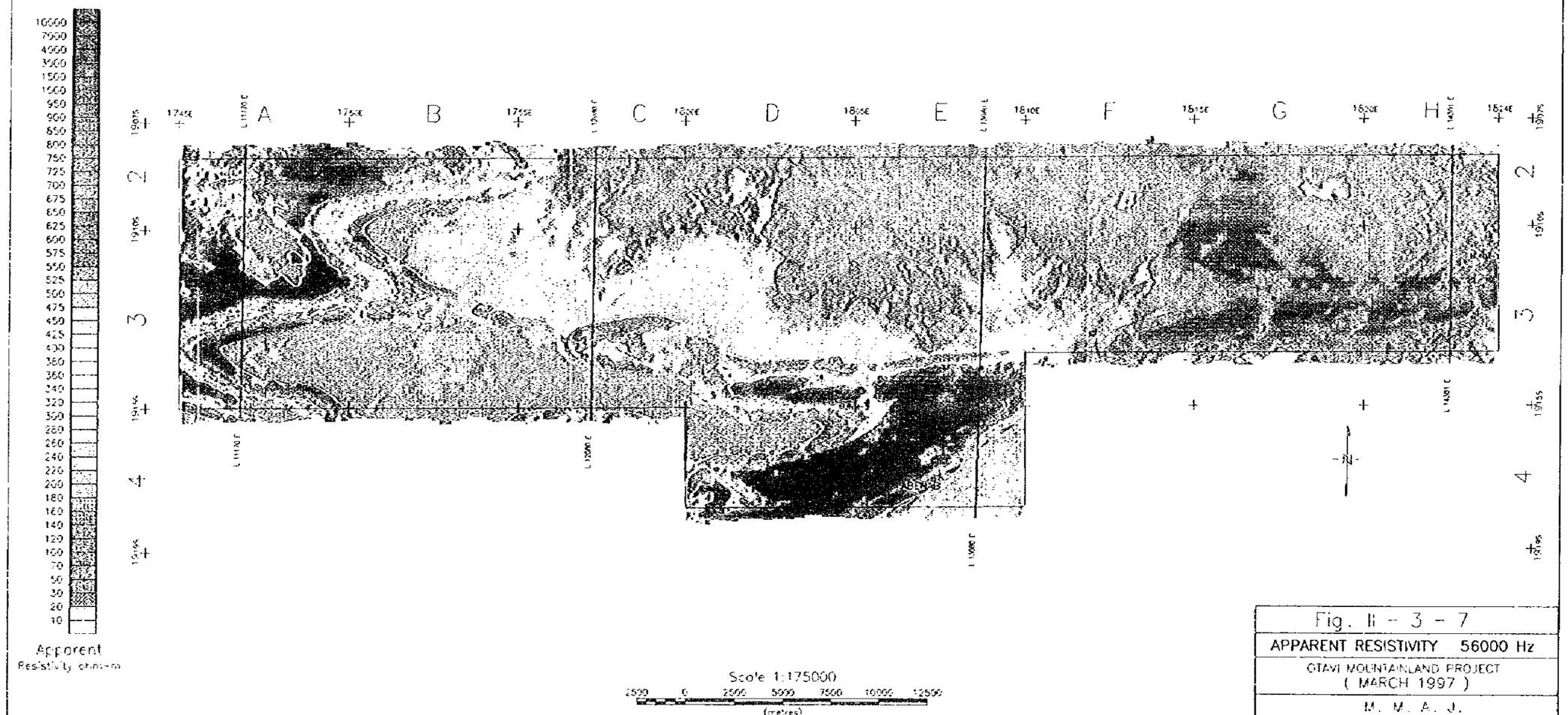

Fig. II - 3 - 7

APPARENT RESISTIVITY 56000 Hz

OTAVI MOUNTAINLAND PROJECT
(MARCH 1997)

M. M. A. J.

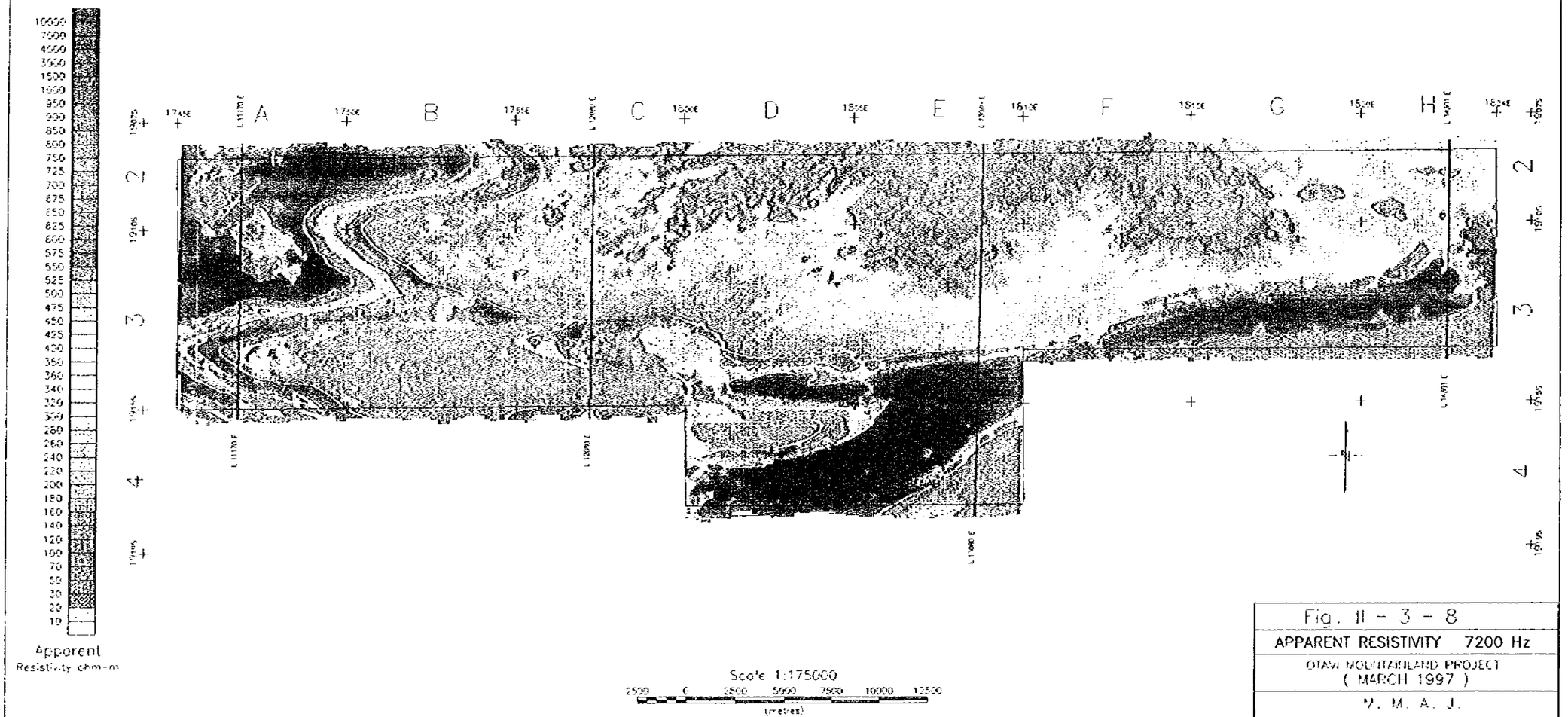

Fig. II - 3 - 8

APPARENT RESISTIVITY 7200 Hz

OTAVI MOUNTAINLAND PROJECT
(MARCH 1997)

M. M. A. J.

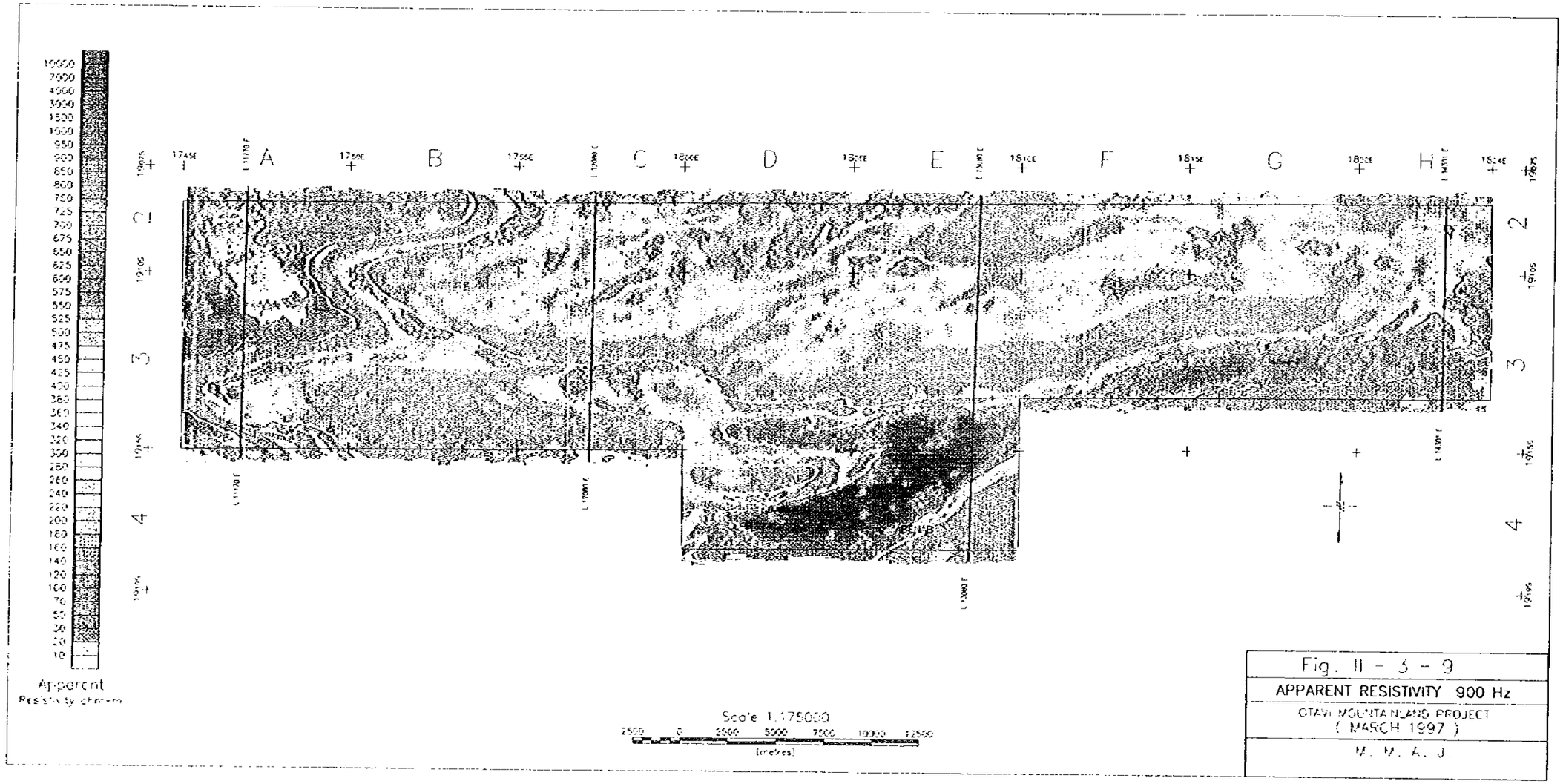

Fig. II - 3 - 9

APPARENT RESISTIVITY 900 Hz

OTAVI MOUNTAINLAND PROJECT
(MARCH 1997)

M. M. A. J.

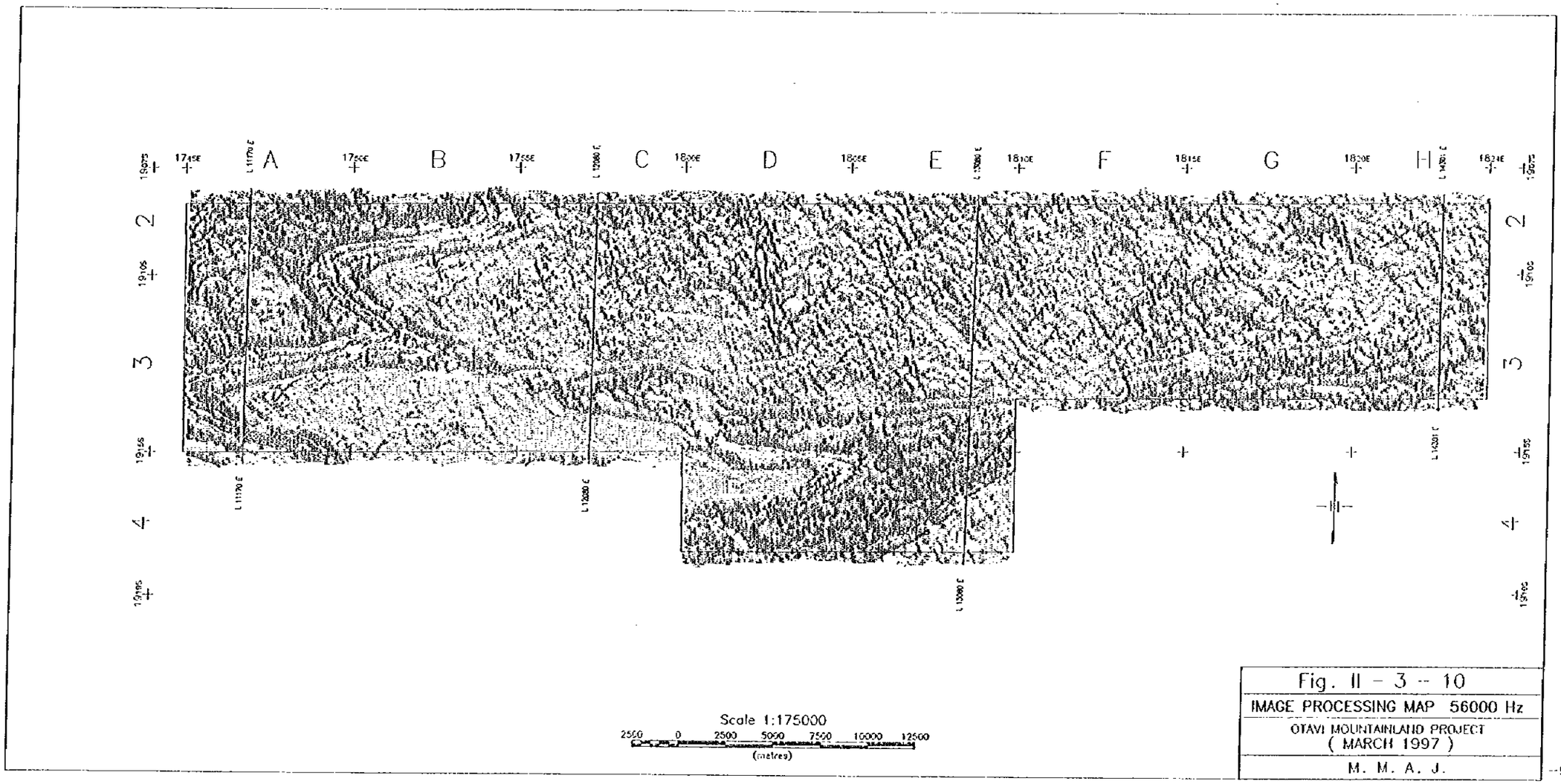

Fig. II - 3 -- 10

IMAGE PROCESSING MAP 56000 Hz

OTAVI MOUNTAINLAND PROJECT
(MARCH 1997)

M. M. A. J.

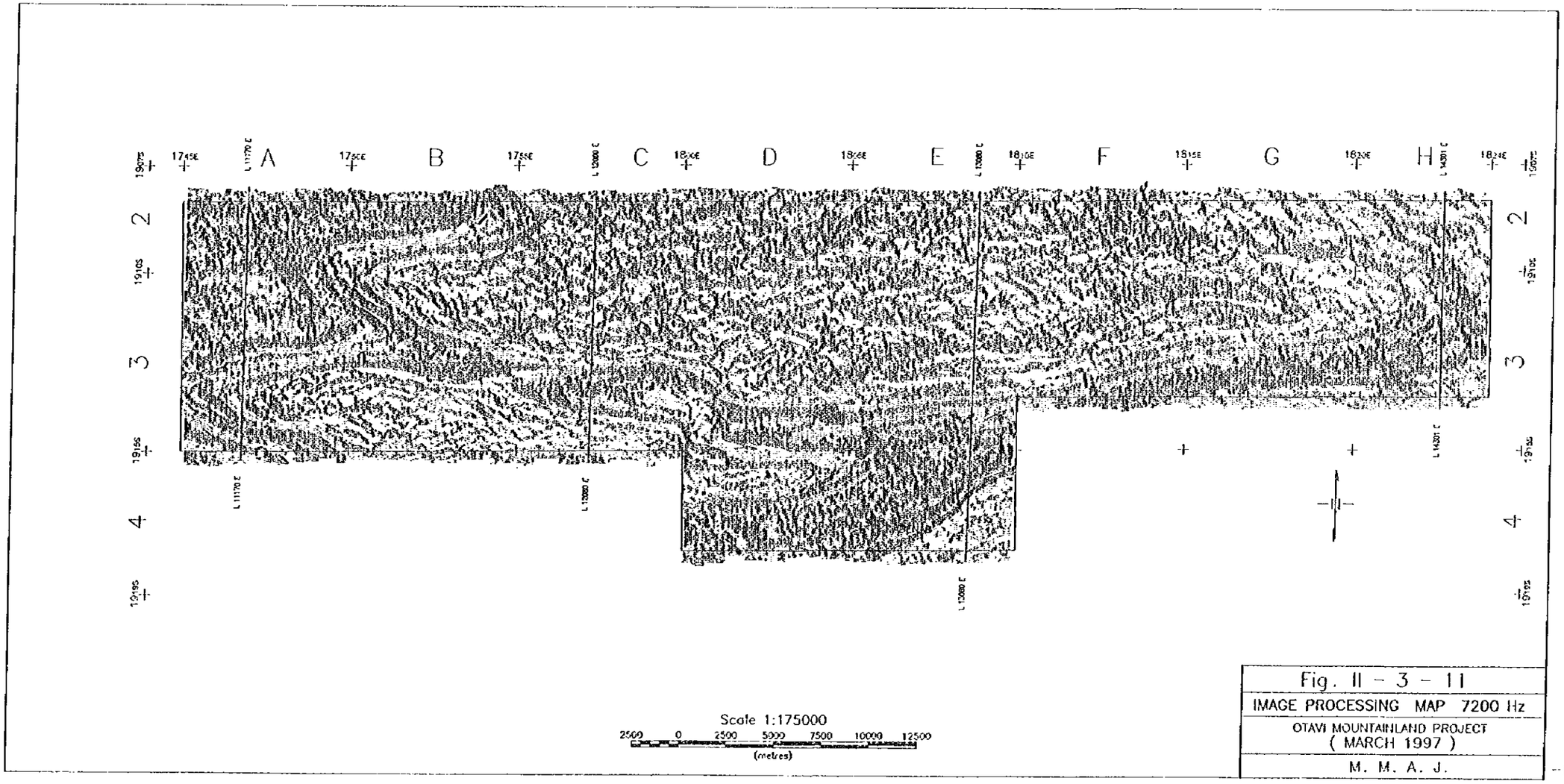

Fig. II - 3 - 11

IMAGE PROCESSING MAP 7200 Hz

OTAVI MOUNTAINLAND PROJECT
(MARCH 1997)

M. M. A. J.

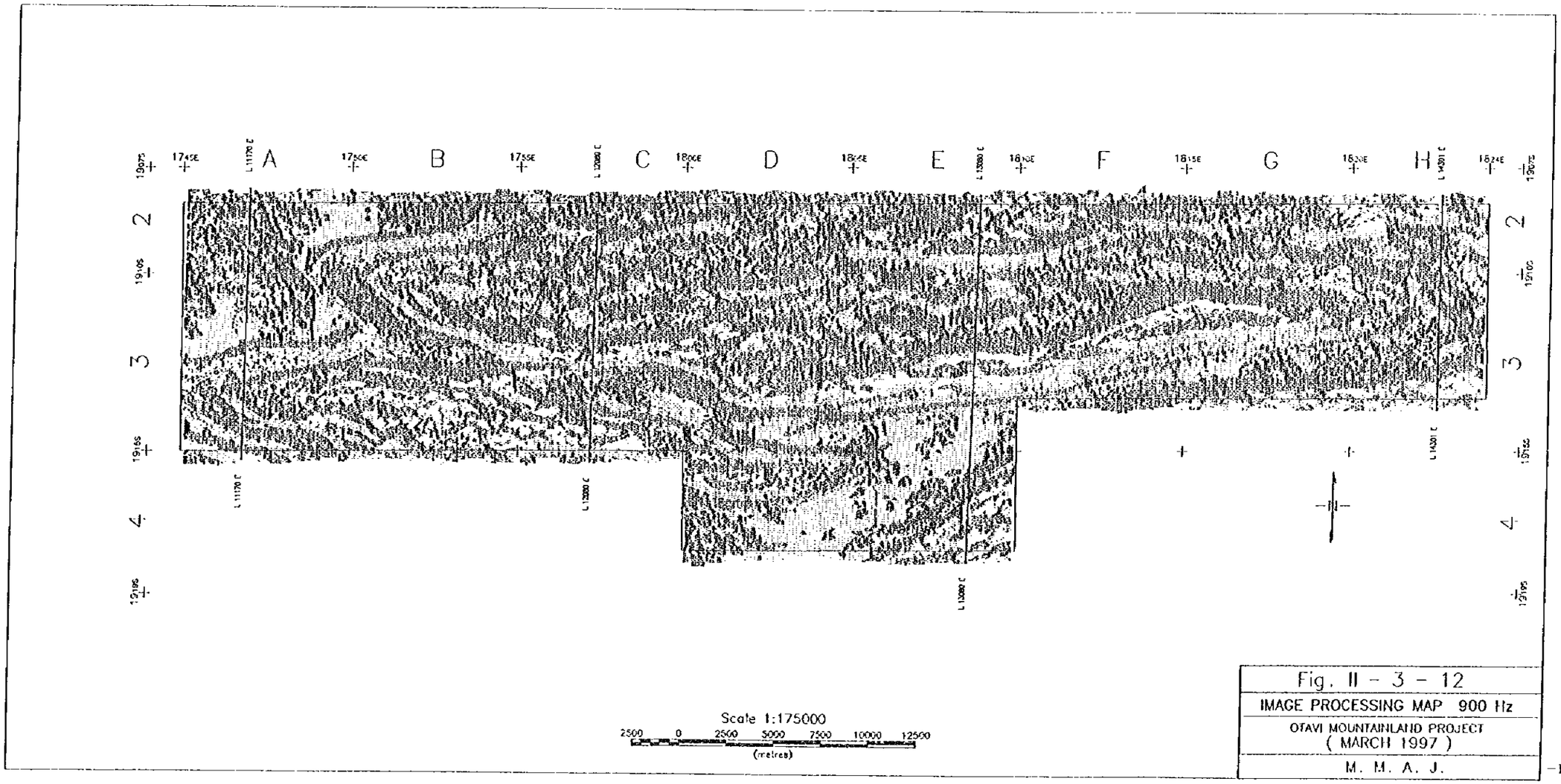

Fig. II - 3 - 12

IMAGE PROCESSING MAP 900 Hz

OTAVI MOUNTAINLAND PROJECT
(MARCH 1997)

M. M. A. J.

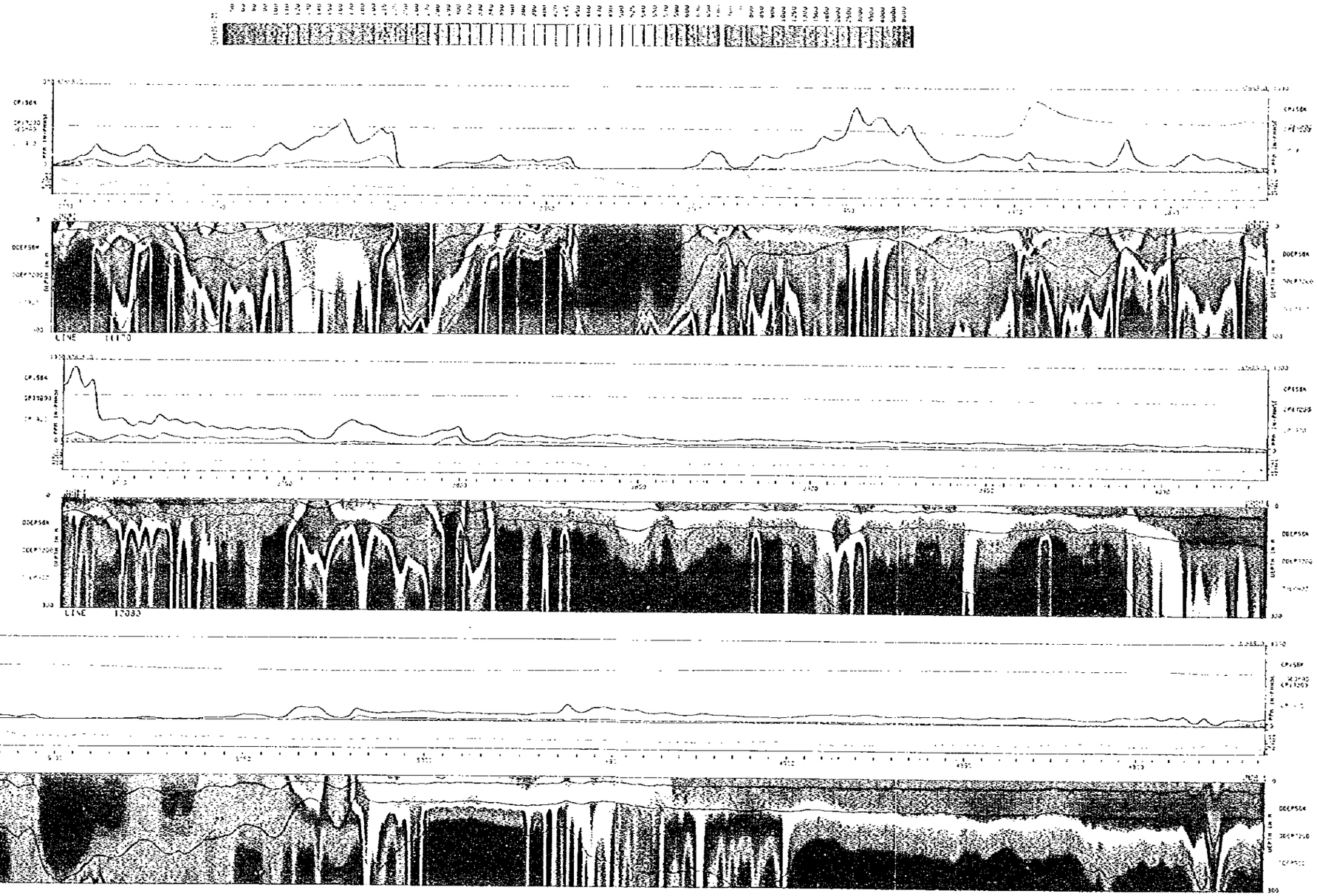

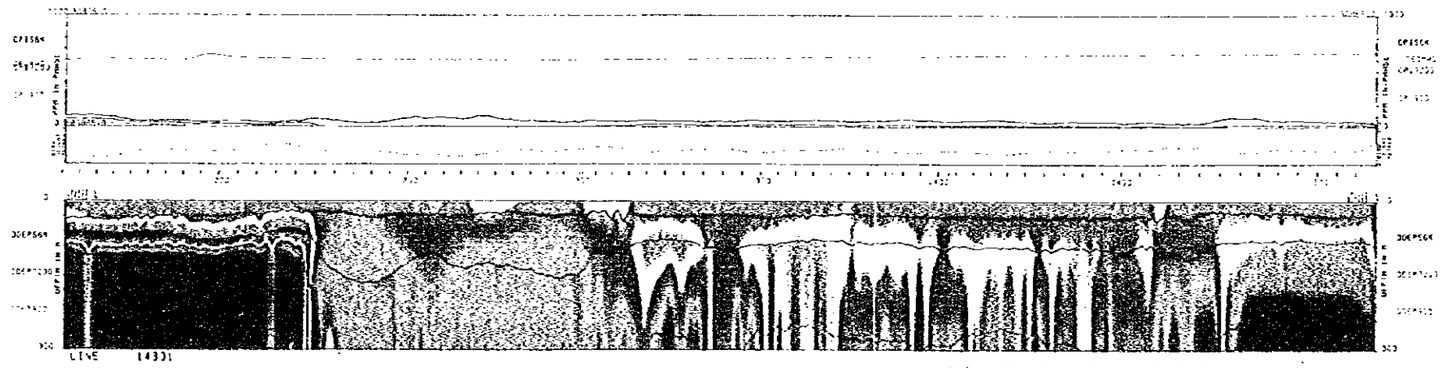

1000 0 1000 2000 3000
(metres)

Fig. II - 3 - 13 Resistivity cross sections

II-3-5-3. Interpretation for resistivity, 900Hz (Fig.II-3-9, Fig.II-3-12)

(1) Total trend of the resistivity is the same as for 56000Hz and 7200 Hz. It provides the deepest information of the survey area. The penetration depth is greater than 300 m in the high resistivity terrain of some thousands of ohm-m, and about 150 m when the low resistivity zone of 100 Ω・m extends from the surface. Some 200 to 300 m penetration is expected when the high resistivity zone is 100 m thick and a low resistivity zone underlies it.

(2) The obvious extension of the low resistivity which corresponds to the Mulden group mentioned in II-3-5-2(3) is recognized in the eastern and central portions of the survey area.

(3) Some northwest striking faults are present in sections E2 and D3 where they are coinciding with aeromagnetic lineaments caused by dolerite dykes associated with the faults. Some other lineaments not association with aeromagnetic anomalies also occur and the electromagnetic image map enhances these.. Neither the map for 56000Hz nor the 7200Hz map show these lineaments. This implies that the lineaments are deep-seated fractures with no surface manifestations. In the east of the survey area, the fractures displace the Mulden group rocks the south.

(4) From block C2 to F2, east-west orientated low resistivity lineaments are observed. These are interpreted as being the lower Mulden just above the unconformity or alternately a low resistivity band within the upper Tsumeb subgroup.

II-3-6. Discussion

II-3-6-1. Resistivity and electromagnetic features of lithofacies

(1) Calcrete

The surficial calcrete is compact and the measurements on the cores give high resistivity of 1500 Ω・m. The lower calcrete facies sometimes include pebbles which results in low resistivity. The electromagnetic data does not distinguish the stratigraphic position and the results range between medium to high resistivity of 500 to 1000 Ω・m. Irregular shaped anomalies shown on the 56000Hz map may indicate lithological inhomogenuity or the presence of ground water rather than a fracture zone cutting the calcrete.

(2) Mulden group

The Mulden Group in the core of the east west trending syncline has a considerable low resistivity varying from 50 to 150 Ω・m.

(3) Upper Tsumeb-subgroup

The pelite bearing lithofacies assigned to the upper Tsumeb group shows low resistivity of 100 Ω・m with local 10 Ω・m from the surface to the depths. The host rock of the Tsumeb and Kombat ore pipes is dolomite underlain by pelitic beds and these are therefore used as a marker horizon in the interpretation.

(4) Dolomites of the Tsumeb subgroup

These dolomites have the highest resistivity ranging from 1000 to 10000 Ω・m. It is suggested that the shallow layer shows higher resistivity than those at depth.

(5) Shallow-seated basement complex

The shallow seated basement complex occurring in the south of the survey area are recognized by a remarkably low resistivity layer underlying the thin calcrete with a high resistivity of 1000 Ω・m. The apparent resistivity at 900 Hz ranges from 15 to 40 Ω・m. The contact between the Damara system and the basement complex is coinciding with the contact delineated by the aeromagnetic survey. This suggest that it is a faulted contact. The cross section reveals that the low resistivity layer is 50 m thick which is underlain by unaltered high resistivity basement complex.

II-3-6-2. Ground water and aquifer

The resistivity of ground water, which was measured in situ, is constant over the survey area with values of about 10 Ω・m and a conductivity 1 mS/cm. These values are lower than those expected for ground water and it is suggested that the water rich in salts. The ground water is filling the cavities in dolomite and calcrete and this will produce a low resistivity similar to sulphide ores. A small-sized low resistivity zone of 200 to 300 Ω・m, located in the thick calcrete terrain and evident only on the 56000 Hz image, may be attributed to a ground water reservoir.

II-3-6-3. Exploration targets

Areas that show overall high resistivity may host potential massive sulphide ore deposit. The exploration target thus is an isolated low resistivity zone within the high resistivity upper dolomites of the Tsumeb subgroup. A strong electromagnetic response would thus be expected in this model. However, it is difficult to distinguish the difference between the response of a potential ore deposit from that of ground water as aquifers of low resistivity can have various shapes.

The dolomites underlying the Mulden group are believed to be favourable hostrock for the Tsumeb-Kombat type ore deposits. However, the Mulden group has uniform low resistivity and the detection of a low resistivity anomalies within it will be difficult. Low resistivity anomalies were thus targeted for follow up work.

(1) Low resistivity lineaments

One target area measuring about 8 km in length and 0.5 to 1 km in thickness is evident in the 7200Hz image and is described in II-3-5-2(6). This low resistivity zone covers the upper Tsumeb subgroup which is the favourable host rock for ore deposit formation. The resistivity decreases at the intersection of the fold axis (200 to 300 Ω・m at the depth of 100 to 200 metres).

(2)Low resistivity zones coinciding with aeromagnetic anomalies occurring in the proximity of the unconformity

The northern limb of the synclines in the west of the survey area as shown on the 7200 and 900 Hz images, shows low resistivity which is coinciding with a broad aeromagnetic anomaly zone that has the order of 20nT.

(3)Isolated spots of low resistivity related to Abenab West-type ore deposit

Some low resistivity zones or spots which seem to branch out from the low resistivity lineament were recognized in the vicinity of MJNM-1 where MVT mineralisation was encountered. These may be indicative of Abenab West-type ore potential. Some of the above mentioned targets coincide with each other thus reinforcing the potential for ore. The favourable targets for further exploration are shown in Fig.II-4-1.

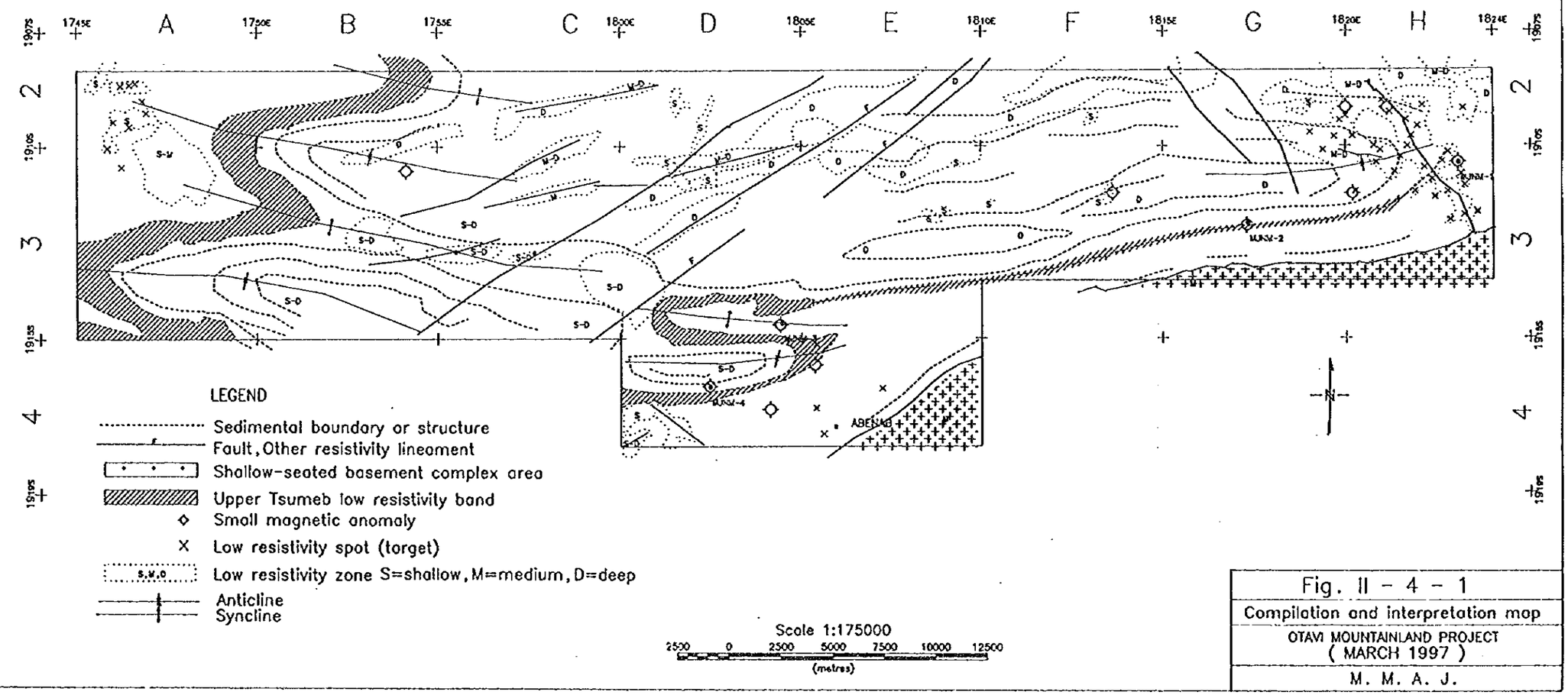

Fig. II - 4 - 1

Compilation and interpretation map

OTAVI MOUNTAINLAND PROJECT
(MARCH 1997)

M. M. A. J.

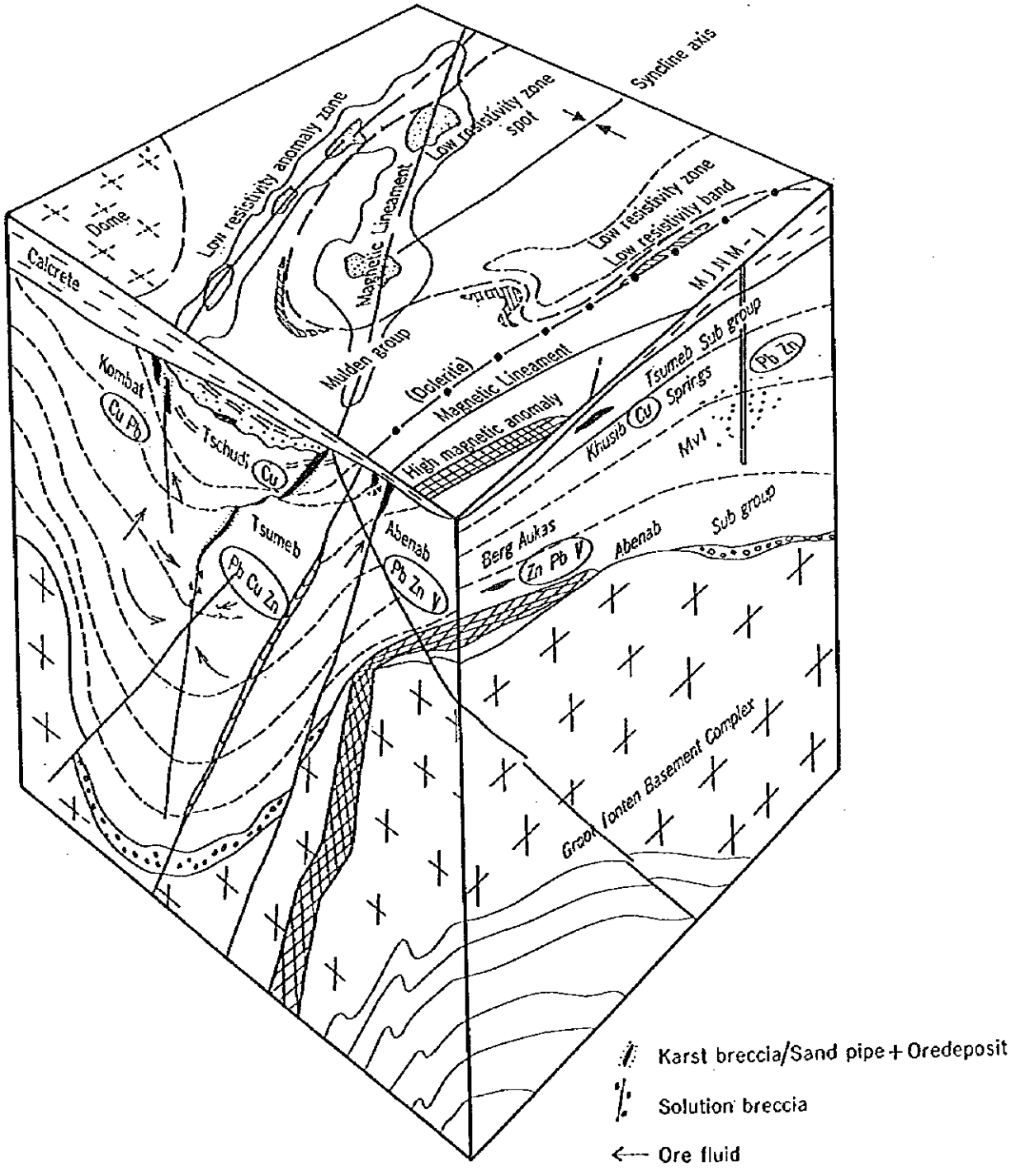

Fig. II - 4 - 2 Model for geological setting, ore deposits and airborne geophysical anomalies

Chapter 4 Compilation and Interpretation

The comprehensive interpretation and discussion of the result of Phase I survey together with that of Phase II survey are presented in Fig.II-4-1. The lead and zinc mineralisation of low to medium ore grade intersected by the Phase II drilling programme showed no characteristically potential structure such as karst breccia and dissolution breccia that are associated with the Tsumeb-Kombat type ore pipes. It also differs from this type by its main sulphide assemblage. Microscopic identification revealed that the host rock was mostly grainstone and had been subjected to dolomitization followed by silicification which is associated with sulphide mineralisation. The mineralisation is thus considered to be of classic Mississippi Valley-type ore deposit.

Literature reports that some potential MVT mineralisation is hosted in dolomite from the Gauss Formation of Abenab Subgroup through to the Huttenberg Formation of Tsumeb Subgroup, and particularly in the grainite of the Elandshoek Formation(T5) and the Huttenberg Formation(T6). The host rock for the mineralisation of MJNM-1 is correlated to T6.

The resistivity maps produced from the airborne electromagnetic survey correlate to the geological maps. The area surveyed during Phase II is mainly underlain by calcrete, the Mulden group, dolomites of the Tsumeb or Abenab subgroups and the basement complex. The shales and aquifers within the calcrete form a low resistivity zone and the massive dolomite and the basement form the high resistivity zone. The shale embedded within dolomite forms a marker horizon which is used to delineate covered geological structures on the resistivity images. The local low resistivity anomaly zones which cross cut the geological trends are important exploration targets as these zones may represent faults and fracture zones associated with massive sulphide mineralisation.

The physical property measurement from the core samples revealed that a low grade lead and zinc mineralisation as intersected in MJNM-1 of Phase II is unlikely to be detected as a low resistivity anomaly. If the mineralisation is of Tsumeb or Kombat type, which includes large amounts of chalcocite and chalcopyrite, it could well give a low resistivity response to electromagnetic signals. The origin of the isolated magnetic anomalies, which were targeted for drilling during Phase II, are believed to be due to iron oxides in a red argillaceous zone of dolomite. This suggests that isolated magnetic anomaly may not necessarily be effective for the search of a Tsumeb/Kombat-type ore deposit.

The Phase II drilling survey confirmed the potential of classic Mississippi Valley-type deposits as well as massive sulphide pipes within the survey area. Massive sulphide deposits have been the exploration target from the start but, this type is not expected to be responsive to geophysical survey in areas with a thick overburden of calcrete.

The helicopter borne electromagnetic survey delineated the subsurface Mulden group. The exploration will thus focus on the Mulden group as possible host to Tsumeb/Kombat-type massive

sulphide deposits. Further exploration is recommended with emphasis placed on the aeromagnetic and low resistivity anomaly zones which traverse the geological trend of the Mulden group. A model for geological setting, ore deposits and airborne geophysical anomalies was prepared for Phase III programme on the basis of the survey result as of Phase II. The model is illustrated in Fig. II-4-2.

Part III Conclusion and Recommendation

Part III Conclusion and Recommendation

Chapter 1 Conclusion

The Phase II survey included an airborne electromagnetic survey, drilling and determining the geophysical properties of the drill cores. The conclusions are discussed in details below:

1. Four drill holes were sunk targeting massive sulphide ore bodies of Tsumeb/Kombat-type. From aeromagnetic anomalies delineated during Phase I

Borehole MJNM-1 intersected low grade, disseminated .lead and zinc mineralisation.

2. The mineralisation showed an average grade of 0.23% lead and 0.38% zinc over 9.16m. The mineralised portions showing more than 1 percent over 9.16 metres, are as follows.

111.58m-111.69m(0.11m)	Pb=1.45%	
112.30m-112.62m(0.32m)	Pb=4.52%	Zn=1.58%
245.75m-246.25m(0.50m)		Zn=1.76%
246.25m-246.65m(0.40m)		Zn=2.28%

3. Microscopic occurrences and chemical assays indicate that the mineralisation formed in a similar way to Mississippi Valley-type ore deposits.

4. No specific relationship between the mineralisation and aeromagnetic anomalies is recognized.

5. Geophysical properties of core samples suggested that the mineral occurrence of this type would give very poor resistivity response to electromagnetic signals.

6. The electromagnetic survey produced three resistivity maps that correspond to the different depths. The results indicate lithological contrast and the general trend of geology. A local low resistivity anomaly zone within an overall high resistivity zone which in turn is transected by the geological trend is considered to be an important locality for potential massive sulphide pipe emplacement. The significance is enhanced by a coinciding aeromagnetic lineament.

7. The favourable area for further exploration during Phase III were targeted. The target area is situated to the west of borehole MJNM-1 and extends some

8 kilometre from east to west and 5 kilometre from north to south. It includes farms Guinab 277, Aris 283 and Vogelsang 284.

Chapter 2 Recommendation for Phase III programme

Based on the results of this survey and interpretation of all data available, the following exploration programme is proposed for Phase III.

III-2-1. Survey area

The proposed survey area is shown in Fig.III-4-1. It is located in the east side of the Phase II survey area and covers farms Guinab 277, Aris 283 and Volgelsang 284. It size is 8 kilometres from

east to west and 5 kilometres from north to south.

III-2-2. Exploration method

Drilling is proposed to following up on the Phase II survey targeting the airborne electromagnetic anomalies. The proposed depth of each holes is 300 metres. The first 80m are mostly calcrete with no economic potential and will thus be percussion drilled.

Bibliography

Beukes N.J.(1996): Carbonate sedimentology. Geol.Soc.Namibia.

Corner B.(1983): An Interpretation of the Aeromagnetic Data Covering the Western Portion of the Damara Orogen in South West Africa/Namibia Spec. Publ.geol.Soc.S.Afr., 11(1983),339-354

Corner B.and W.A.Wilsher(1987):Proceedings of Exploration '87:Third Decennial In Geophysical and Geochemical Exploration for Minerals and Ground water, edited by G.D.Garland, Ontario Geological Survey, Special Volume 3, 960 p.

De Beer,J.H.et al(1982):Magnetometer array and deep Schlumberger soundings in the Damara orogen belt, South West Africa.Geophys. J.R.astr. Soc.,70,1982.11-29p.

Geological Survey of Namibia(1982):The Geology of South West Africa Namibia 1:1000000

Geological Survey of Namibia(1988):Geological Map of the Damara Orogen South West Africa/Namibia-1988 1:500 000

Geological Survey of Namibia(1993):Aeromagnetic Anomaly Map of Namibia 1: 1 000 000

Huang H. and Fraser D.C.(1996): The differential parameter method for multi-frequeny airborne resisitvity mapping. Geophysics, vol.61,No.1 p.100-109

Innes J. and Chaplin R.C.(1986):Ore Bodies of the Kombat Mine, South West Africa /Namibia. Mineral Deposits fo Southern Africa(1986),1789-1805p.

Japan International Cooperation Agency and Metal Mining Agency of Japan(1996): Reort on the Mineral Exploration in the Otavi Montainland Area the Republic of Namibia Phase I (1996)

Japan Mining Engineering Center for International Cooperation(1992):Report on Project finding Survey-Satellite Image Interpretation, Republic of Namibia 1992 (in Japanese)

Japan Mining Engineering Center for International Cooperation(1992):Report on Project finding Survey-Information Analysis, Republic of Namibia 1992 (in Japanese)

Kileen P.G.(1979):Gamma Ray Spectrometric Methods in Uranium Exploration - Appli cation and Interpretaion. Exploration '87 Proceedings-Geophysical Methods, Advances in the State of the Art. Geological Survey of Canada, Economic Geology Report 31,163-229p.,1979

Killick A.M.(1986):A Review of the Economic Geology of Northern South West Africa/Namibia. Mineral Deposits fo Southern Africa(1986),1709-1717p.

Kimura S.(1987):Localization of Spa using Surface Gamma-Ray Radiometric

Exploration Spa Science Vol. 37 1987 73-92p. (in Japanese)

Leach D.L. and Sangster D.F. (1993):Mississippi Valley-type Lead-Zinc Deposits Kirkham, R.V. et al eds., Mineral Deposit Modeling: Geol. Assoc. Canada, Spec. Pap. 40, 289-314p.

Lombaard A.F., Gunzel A., Innes J. and Kruger T.L. (1986):The Tsumeb Lead-Copper-Zinc-Silver Deposit, South West Africa/Namibia. Mineral Deposits fo Southern Africa(1986), 1761-1787p.

Miller R.McG. (1983):Economic Implications of Plate Tectonic Models of the Damara Orogen. Spec. Publ. Geol. Soc. S. Afr., 11(1983), 385-395p.

Mining Journal :Country Supplement NAMIBIA Vol. 319 No. 8196 1992

Miller R.McG. (1994):The Mineral Resources of Namibia ---Mineral Exploration Targets

Niall M. and McMaus C. (1994):Proterozoic Crustal & Metallogenic Evolution. Abstracts. Geological Society & Geological Survey of Namibia

Palacky G.J. (1986): Geological background to resistivity nmapping. Geol. Sur. Canada, Paper 86-22, p. 19-27, 1986

Tompkins et al. (1994):The Cadjebut as an Example of Mississippi Valley-Type Mine ralization on the Lennard Shelf, Western Australia-Single Episode or Multiple Events? Econ. Geol., vol. 89. No. 3, 1994, 467-492p.

Tsumeb Corporation Limited(1995):Kombat Mine 1995

Weike H.J., Allsopp H.L. and Huges M.J. (1983):Lead Isotopic Studies Relating to the Genesis of the Base-Metal Deposits in the Owambo Basin, Namibia Spec. Publ. Geol. Soc. S. Afr., 11(1983), 321p.

Wolf K.H. edit. (1985):Handbook of Strata-Bound and Stratiform Ore Deposits, Vol. 5 Regional Studies, Vol. 6 Cu Zn Pb and Ag Deposits, Vol. 13 Regional Studies and Specific Deposits, ELSEVIER